Inorg. Chem. **2009**, *48*, 2114−2127

What a Difference a 5f Element Makes: Trivalent and Tetravalent Uranium Halide Complexes Supported by One and Two Bis[2-(diisopropylphosphino)-4-methylphenyl]amido (PNP) Ligands

Thibault Cantat, Brian L. Scott, David E. Morris,* and Jaqueline L. Kiplinger*

Los Alamos National Laboratory, Los Alamos, New Mexico 87545

Received October 27, 2008

The coordination behavior of the bis[2-(diisopropylphosphino)-4-methylphenyl]amido ligand (PNP) toward $UI_3(THF)_4$ and UCl_4 has been investigated to access new uranium(III) and uranium(IV) halide complexes supported by one and two PNP ligands. The reaction between (PNP)K (**6**) and 1 equiv of $UI_3(THF)_4$ afforded the trivalent halide complex (PNP)UI_2(4-^{t}Bu-pyridine)$_2$ (**7**) in the presence of 4-tert-butylpyridine. The same reaction carried out with UCl_4 and no donor ligand gave $[(PNP)UCl_3]_2$ (**8**), in which the uranium coordination sphere in the (PNP)UCl_3 unit is completed by a bridging chloride ligand. When UCl_4 is reacted with 1 equiv (PNP)K (**6**) in the presence of THF, trimethylphosphine oxide (TMPO), or triphenylphosphineoxide (TPPO), the tetravalent halide complexes (PNP)UCl_3(THF) (**9**), (PNP)UCl_3(TMPO)$_2$ (**10**), and (PNP)UCl_3(TPPO) (**11**), respectively, are formed in excellent yields. The bis(PNP) complexes of uranium(III), $(PNP)_2UI$ (**12**), and uranium(IV), $(PNP)_2UCl_2$ (**13**), were easily isolated from the analogous reactions between 2 equiv of **6** and $UI_3(THF)_4$ or UCl_4, respectively. Complexes **12** and **13** represent the first examples of complexes featuring two PNP ligands coordinated to a single metal center. Complexes **7**-**13** have been characterized by single-crystal X-ray diffraction and ^{1}H and ^{31}P NMR spectroscopy. The X-ray structures demonstrate the ability of the PNP ligand to adopt new coordination modes upon coordination to uranium. The PNP ligand can adopt both *pseudo*-meridional and *pseudo*-facial geometries when it is κ^3-(*P*,*N*,*P*) coordinated, depending on the steric demand at the uranium metal center. Additionally, its hemilabile character was demonstrated with an unusual κ^2-(*P*,*N*) coordination mode that is maintained in both the solid-state and in solution. Comparison of the structures of the mono(PNP) and bis(PNP) complexes **7**, **9**, **11**-**13** with their respective C_5Me_5 analogues **1**-**4** undoubtedly show that a more sterically congested environment is provided by the PNP ligand. The electronic influence of replacing the C_5Me_5 ligands with PNP was investigated using electronic absorption spectroscopy and electrochemistry. For **12** and **13**, a chemically reversible wave corresponding to the U^{IV}/U^{III} redox transformation comparable to that for **3** and **4** was observed. However, a ∼350 mV shift of this couple to more negative potentials was observed on substitution of the bis(C_5Me_5) by the bis(PNP) framework, therefore pointing to a greater electronic density at the metal center in the PNP complexes. The UV−visible region of the electronic spectra for the mono(PNP) and bis(PNP) complexes appear to be dominated by PNP ligand-based transitions that are shifted to higher energy in the uranium complexes than in the simple ligand anion (**6**) spectrum, for both the U^{VI} and U^{III} oxidation states. The near IR region in complexes **1**−**4** and **7**, **9**, **11**−**13** is dominated by f-f transitions derived from the $5f^3$ and $5f^2$ valence electronic configuration of the metal center. Though complexes of both ligand sets exhibit similar intensities in their f-f bands, a somewhat larger ligand-field splitting was observed for the PNP system, consistent with its higher electron donating ability.

Introduction

Non-aqueous chemistry of the actinides has proved invaluable for gaining insight into the behavior and properties of these elements in a variety of chemical environments. These can range from inert atmosphere syntheses of well-defined actinide materials for nuclear fuel applications and materials science[1,2] to addressing purely fundamental questions such as the involvement of 5f-orbitals in bonding and reactivity by studying highly reactive actinide molecular complexes

* To whom correspondence should be addressed. E-mail: kiplinger@lanl.gov.

10.1021/ic802061x CCC: $40.75
Published on Web 01/23/2009

Chart 1. Alternatives to Cyclopentadienyl Ligands Employed to Support Non-Aqueous Actinide Chemistry[17]

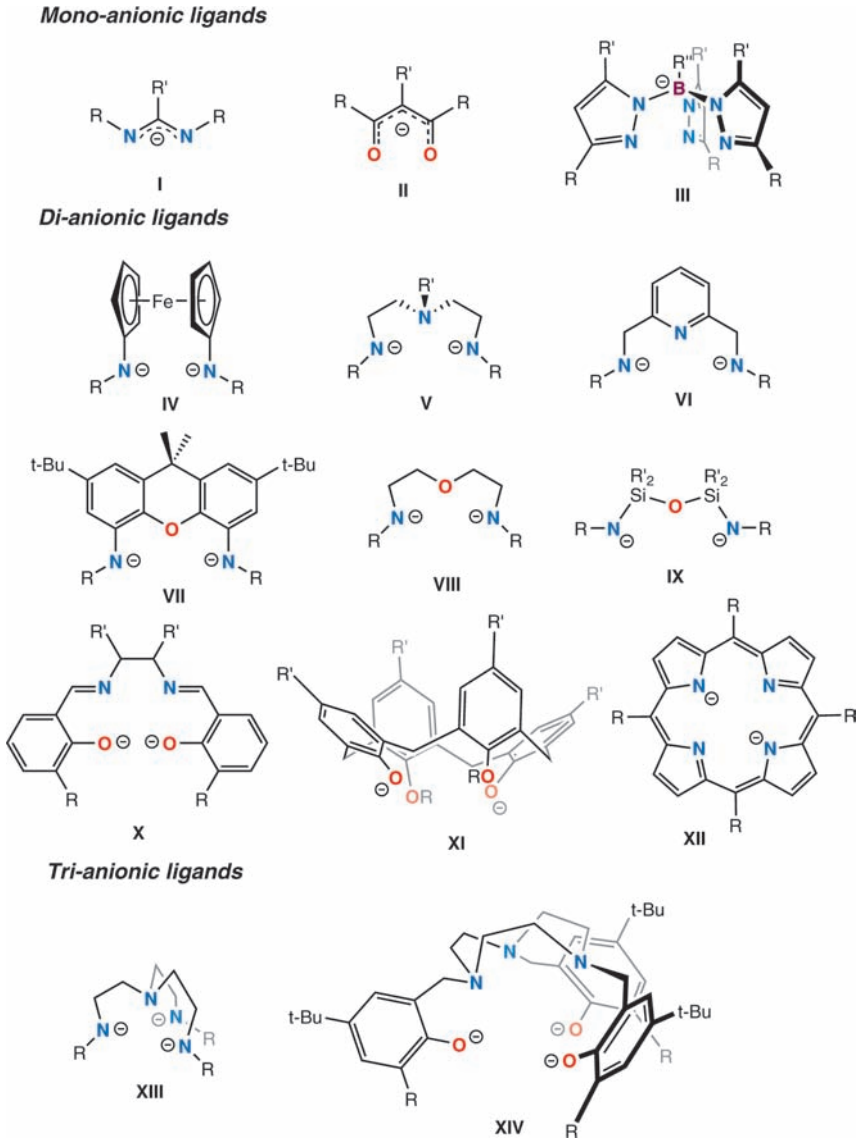

in the absence of air and water.[3−13] The synthesis of uranium nitride/carbide materials and coordination complexes featuring tetravalent, pentavalent, and hexavalent uranium−main group element multiple bonds (i.e., oxo, imido, and phosphinidene complexes) represent major achievements in this area.[14,15]

The optimal ligand sets for supporting non-aqueous actinide chemistry must not only coordinate to the metal and stabilize the complex against disproportionation and dissociation reactions but also support a variety of oxidation states. Because of the large ionic radii of the actinides, the ligand framework should also bring enough steric bulk and electronic saturation so that only a few controlled coordination sites remain available for chemistry. For these reasons, the bis(pentamethylcyclopentadienyl) $(C_5Me_5)_2$ and the tris(cyclopentadienyl) $(C_5H_5)_3$ ligand sets have been enormously successful as frameworks for organometallic actinide chemistry.[15,16]

In recent years, new heteroatom-based ligand sets spanning a broad range of coordination modes have emerged (Chart 1) and some have been shown to support reactivity patterns and structures that are not currently available for the cyclopentadienyl systems.[17] On the basis of the electropositive nature of the actinides, these supporting ligands were all designed using hard donor atoms (oxygen and nitrogen). Mono-, di- and trianionic backbones with denticity of up to

(1) Arai, Y.; Morihira, M.; Ohmichi, T. *J. Nucl. Mater.* **1993**, *202*, 70–78.
(2) Berthold, H. J.; Knecht, H. *Angew. Chem., Int. Ed.* **1965**, *4*, 433–434.
(3) Arnold, P. L.; Patel, D.; Wilson, C.; Love, J. B. *Nature* **2008**, *451*, 315–318.
(4) Brennan, J. G.; Green, J. C.; Redfern, C. M. *J. Am. Chem. Soc.* **1989**, *111*, 2373–2387.
(5) Cantat, T.; Graves, C. R.; Jantunen, K. C.; Scott, B. L.; Schelter, E. J.; Burns, C. J.; Hay, P. J.; Morris, D. E.; Kiplinger, J. L. *J. Am. Chem. Soc.* **2008**, *130*, 17537–17551.
(6) Diaconescu, P. L.; Cummins, C. C. *J. Am. Chem. Soc.* **2002**, *124*, 7660–7661.
(7) Evans, W. J.; Kozimor, S. A.; Ziller, J. W.; Kaltsoyannis, N. *J. Am. Chem. Soc.* **2004**, *126*, 14533–14547.
(8) Graves, C. R.; Yang, P.; Kozimor, S. A.; Vaughn, A. E.; Clark, D. L.; Conradson, S. D.; Schelter, E. J.; Scott, B. L.; Thompson, J. D.; Hay, P. J.; Morris, D. E.; Kiplinger, J. L. *J. Am. Chem. Soc.* **2008**, *130*, 5272–5285.

six have been used to tune the number of remaining reactive sites on the metal center. Among these, the tris(pyrazolylborate) ligand (**III**), which is considered the inorganic complement of $C_5Me_5^-$, has been utilized the most in supporting coordination chemistry for both uranium(III) and uranium(IV) with one and two ligands coordinated to the metal ion. However, a major drawback of the tris(pyrazolylborate) system is its vulnerability to fragmentation reactions (cleavage of the B−N bonds) when coordinated to highly electropositive metals.[18−21] On the whole, none of these ligands has met with the same success as the cyclopentadienyl-based systems.[15,22]

Ligands that combine both hard and soft coordination environments have proved useful for stabilizing highly reactive functional groups such as alkylidenes, phosphinidenes, and imides on transition metals and lanthanides.[23−30] However, soft donor ligands have been largely ignored as supporting ligands for early actinide chemistry, with the exception of coordination complexes featuring phosphorus and chalcogenide ligands prepared to investigate actinide/lanthanide separation technologies and questions about covalency in "hard-soft" interactions.[31−37] Given that soft donor ligands provide an excellent opportunity to promote the low valent chemistry of uranium, we initiated a program to develop the coordination chemistry of the robust monoanionic bis[2-(diisopropylphosphino)-4-methylphenyl]amido or PNP ligand toward the uranium halide complexes, UCl_4, and $UI_3(THF)_4$. Herein, we report the synthesis and characterization of a series of uranium(III) and uranium(IV) halide complexes supported by one and two PNP ligands and discuss the structural and electronic consequences of replacing the pentamethylcyclopentadienyl (C_5Me_5) ligand by the softer PNP ligand.

Experimental Section

Instrumentation and Sample Protocols. Electronic absorption spectral data were obtained for toluene solutions of the complexes over the wavelength range from 280−2000 nm on a Perkin-Elmer Model Lambda 950 UV−visible-near-infrared spectrophotometer. Data were collected in 1 mm path length cuvettes loaded in the Vacuum Atmospheres drybox system described below and run versus a solvent reference or versus air. In the latter case, the data were corrected for solvent absorbance post-acquisition. Spectral resolution was 2 nm. Voltammetric data were obtained in the Vacuum Atmospheres drybox system described below. All data were collected using a Perkin-Elmer Princeton Applied Research Corporation (PARC) Model 263 potentiostat under computer control with PARC Model 270 software. All sample solutions were ∼1−2 mM in complex with ∼0.1 M $[Bu_4N][B(3,5\text{-}(CF_3)_2\text{-}C_6H_3)_4]$ supporting electrolyte in THF solvent. All data were collected with

(9) Hayton, T. W.; Boncella, J. M.; Scott, B. L.; Batista, E. R.; Hay, P. J. *J. Am. Chem. Soc.* **2006**, *128*, 10549–10559.
(10) Maynadie, J.; Berthet, J. C.; Thuery, P.; Ephritikhine, M. *J. Am. Chem. Soc.* **2006**, *128*, 1082–1083.
(11) Nocton, G.; Pecaut, J.; Mazzanti, M. *Angew. Chem., Int. Ed.* **2008**, *47*, 3040–3042.
(12) Schelter, E. J.; Wu, R.; Scott, B. L.; Thompson, J. D.; Morris, D. E.; Kiplinger, J. L. *Angew. Chem., Int. Ed.* **2008**, *47*, 2993–2996.
(13) Summerscales, O. T.; Cloke, F. G. *Struct. Bonding (Berlin)* **2008**, *127*, 87–117.
(14) Burns, C. J.; Bursten, B. E. *Comments Inorg. Chem.* **1989**, *9*, 61–93.
(15) Burns, C. J.; Eisen, M. S. In *The Chemistry of the Actinide and Transactinide Elements*, 3rd ed.; Morss, L. R., Edelstein, N. M., Fuger, J., Eds.; Springer: The Netherlands, 2006; Vol. *5*, pp 2799−2910.
(16) Marks, T. J.; Streitwieser, A. In *The Chemistry of the Actinide Elements*, 2nd ed.; Katz, J. J., Seaborg, G. T., Morss, L. R., Eds.; Chapman and Hall: New York, 1986; Vol. *2*, pp 1547−1587.
(17) Representative references for **I**:(a) Wedler, M.; Knosel, F.; Noltemeyer, M.; Edelmann, F. T.; Behrens, U. *J. Organomet. Chem.* **1990**, *388*, 21–45. (b) Muller, M.; Williams, V. C.; Doerrer, L. H.; Leech, M. A.; Mason, S. A.; Green, M. L. H.; Prout, K. *Inorg. Chem.* **1998**, *37*, 1315–1323. (c) Villiers, C.; Thuery, P.; Ephritikhine, M. *Eur. J. Inorg. Chem.* **2004**, 4624–4632. For **II**: (d) Brown, D.; Whittaker, B.; Tacon, J. *J. Chem. Soc., Dalton Trans.* **1975**, 34–39. (e) Baudin, C.; Charpin, P.; Ephritikhine, M.; Lance, M.; Nierlich, M.; Vigner, J. *J. Organomet. Chem.* **1988**, *345*, 263–274. For **III**: (f) Domingos, A.; Marcalo, J.; Santos, I.; Dematos, A. P. *Polyhedron* **1990**, *9*, 1645–1652. (g) Domingos, A.; Marques, N.; Dematos, A. P. *Polyhedron* **1990**, *9*, 69–74. (h) Sun, Y.; McDonald, R.; Takats, J. *Inorg. Chem.* **1994**, *33*, 4433–4434. (i) Silva, M.; Domingos, A.; de Matos, A. P.; Marques, N.; Trofimenko, S. *J. Chem. Soc., Dalton Trans.* **2000**, 4628–4634. (j) Maria, L.; Domingos, A.; Galvao, A.; Ascenso, J.; Santos, I. *Inorg. Chem.* **2004**, *43*, 6426–6434. (k) Enriquez, A. E.; Scott, B. L.; Neu, M. P. *Inorg. Chem.* **2005**, *44*, 7403–7413. For **IV**: (l) Monreal, M. J.; Diaconescu, P. L. *Organometallics* **2008**, *27*, 1702–1706. For **V**: (m) Wilson, D. J.; Sebastian, A.; Cloke, F. G. N.; Avent, A. G.; Hitchcock, P. B. *Inorg. Chim. Acta* **2003**, *345*, 89–94. For **VI** and **VII**: (n) Cruz, C. A.; Emslie, D. J. H.; Harrington, L. E.; Britten, J. F.; Robertson, C. M. *Organometallics* **2007**, *26*, 692–701. (o) Cruz, C. A.; Emslie, D. J. H.; Harrington, L. E.; Britten, J. F. *Organometallics* **2008**, *27*, 15–17. For **VIII** and **IX**: (p) Jantunen, K. C.; Batchelor, R. J.; Leznoff, D. B. *Organometallics* **2004**, *23*, 2186–2193. (q) Jantunen, K. C.; Haftbaradaran, F.; Katz, M. J.; Batchelor, R. J.; Schatte, G.; Leznoff, D. B. *Dalton Trans.* **2005**, 3083–3091. For **X**: (r) Hill, R. J.; Rickard, C. E. F.; White, H. E. *J. Inorg. Nucl. Chem.* **1981**, *43*, 721–726. (s) Le Borgne, T.; Riviere, E.; Marrot, J.; Thuery, P.; Girerd, J. J.; Ephritikhine, M. *Chem.—Eur. J.* **2002**, *8*, 774–783. (t) Salmon, L.; Thuery, P.; Ephritikhine, M. *Dalton Trans.* **2004**, 4139–4145. For **XI**: (u) Old, J.; Danopoulos, A. A.; Winston, S. *New J. Chem.* **2003**, *27*, 672–674. (v) Salmon, L.; Thuery, P.; Asfari, Z.; Ephritikhine, M. *Dalton Trans.* **2006**, 3006–3014. (w) Salmon, L.; Thuery, P.; Ephritikhine, M. *Chem. Commun.* **2006**, 856–858. For **XII**: (x) Dormond, A.; Belkalem, B.; Charpin, P.; Lance, M.; Vigner, D.; Folcher, G.; Guilard, R. *Inorg. Chem.* **1986**, *25*, 4785–4790. (y) Girolami, G. S.; Milam, S. N.; Suslick, K. S. *Inorg. Chem.* **1987**, *26*, 343–344. (z) Korobkov, I.; Gambarotta, S.; Yap, G. P. A. *Angew Chem., Int. Ed.* **2002**, *41*, 3433–3436. For **XIII**: (aa) Scott, P.; Hitchcock, P. B. *Polyhedron* **1994**, *13*, 1651–1653. (bb) Roussel, P.; Hitchcock, P. B.; Tinker, N.; Scott, P. *Chem Commun.* **1996**, 2053–2054. (cc) Roussel, P.; Scott, P. *J. Am. Chem. Soc.* **1998**, *120*, 1070–1071. (dd) Boaretto, R.; Roussel, P.; Kingsley, A. J.; Munslow, I. J.; Sanders, C. J.; Alcock, N. W.; Scott, P. *Chem. Commun.* **1999**, 1701–1702. (ee) Roussel, P.; Alcock, N. W.; Boaretto, R.; Kingsley, A. J.; Munslow, I. J.; Sanders, C. J.; Scott, P. *Inorg. Chem.* **1999**, *38*, 3651–3656. For **XIV**: (ff) Castro-Rodriguez, I.; Nakai, H.; Gantzel, P.; Zakharov, L. N.; Rheingold, A. L.; Meyer, K. *J. Am. Chem. Soc.* **2003**, *125*, 15734–15735. (gg) Castro-Rodriguez, I.; Nakai, H.; Zakharov, L. N.; Rheingold, A. L.; Meyer, K. *Science* **2004**, *305*, 1757–1759. (hh) Castro-Rodriguez, I.; Meyer, K. *J. Am. Chem. Soc.* **2005**, *127*, 11242–11243. (ii) Castro-Rodriguez, I.; Nakai, H.; Meyer, K. *Angew. Chem., Int. Ed.* **2006**, *45*, 2389–2392.
(18) Marques, N.; Sella, A.; Takats, J. *Chem. Rev.* **2002**, *102*, 2137–2159.
(19) Maria, L.; Domingos, A.; Santos, I. *Inorg. Chem. Commun.* **2003**, *6*, 58–60.
(20) Silva, M.; Domingos, A.; de Matos, A. P.; Marques, N.; Trofimenko, S. *J. Chem. Soc., Dalton Trans.* **2000**, 4628–4634.
(21) Domingos, A.; Marques, N.; Dematos, A. P.; Santos, I.; Silva, M. *Organometallics* **1994**, *13*, 654–662.
(22) Ephritikhine, M. *Dalton Trans.* **2006**, 2501–2516.
(23) Ozerov, O. V. In *The Chemistry of Pincer Compounds*; Morales-Morales, D., Jensen, C., Eds.; Elsevier Science: New York, 2007; pp 287−309.
(24) Weng, W.; Yang, L.; Foxman, B. M.; Ozerov, O. V. *Organometallics* **2004**, *23*, 4700–4705.
(25) Bailey, B. C.; Huffman, J. C.; Mindiola, D. J.; Weng, W.; Ozerov, O. V. *Organometallics* **2005**, *24*, 1390–1393.
(26) Liang, L. C. *Coord. Chem. Rev.* **2006**, *250*, 1152–1177.
(27) Mindiola, D. J. *Acc. Chem. Res.* **2006**, *39*, 813–821.
(28) Zhao, G. Y.; Basuli, F.; Kilgore, U. J.; Fan, H. J.; Aneetha, H.; Huffman, J. C.; Wu, G.; Mindiola, D. J. *J. Am. Chem. Soc.* **2006**, *128*, 13575–13585.

the positive-feedback IR compensation feature of the software/potentiostat activated to ensure minimal contribution to the voltammetric waves from uncompensated solution resistance (typically ~1 kΩ under the conditions employed). Solutions were contained in a PARC Model K0264 microcell consisting of a ~3 mm diameter Pt disk working electrode, a Pt wire counter electrode, and a Ag wire quasi-reference electrode. Scan rates from 20−5000 mV/s were employed in the cyclic voltammetry scans to assess the chemical and electrochemical reversibility of the observed redox transformations. Half-wave potentials were determined from the peak values in the square-wave voltammograms. Potential calibrations were performed at the end of each data collection cycle using the ferrocenium/ferrocene couple as an internal standard. Voltammetric and electronic absorption data were analyzed using Wavemetrics IGOR Pro (Version 6.0) software on a Macintosh platform.

General Synthetic Considerations. Unless otherwise noted, all reactions and manipulations were performed at 20 °C in a recirculating Vacuum Atmospheres NEXUS Model inert atmosphere (N_2) drybox equipped with a 40CFM Dual Purifier NI-Train. Glassware was dried overnight at 150 °C before use. All NMR spectra were obtained using a Bruker Avance 300 MHz spectrometer. Chemical shifts for ^{1}H and ^{13}C{^{1}H} NMR spectra were referenced to solvent impurities and ^{31}P{^{1}H} NMR spectra were referenced to pure phosphoric acid. Mass spectrometric (MS) analyses were obtained at the University of California, Berkeley mass spectrometry facility using either a VG ProSpec (EI) or VG70-SE (FAB) mass spectrometer. Elemental analyses were performed at the University of California, Berkeley Microanalytical facility on a Perkin-Elmer Series II 2400 CHNS Analyzer. X-ray crystallographic data were collected on a Bruker D8 diffractometer, with an APEX II charge-coupled-device (CCD) detector and a KRYOFLEX liquid nitrogen vapor-cooling device. Structural solution and refinement was achieved using the SHELXL97 program suite (Table 1).[38] Details regarding data collection are provided in the CIF files.

Unless otherwise noted, reagents were purchased from commercial suppliers and used without further purification. Celite (Aldrich), alumina (Brockman I, Aldrich) and 4 Å molecular sieves (Aldrich) were dried under dynamic vacuum at 250 °C for 48 h prior to use. Hexane (anhydrous, Aldrich), pentane (anhydrous, Aldrich), toluene (anhydrous, Aldrich), tetrahydrofuran (anhydrous, Aldrich), and bis(trimethylsilyl)ether (Aldrich) were dried over KH for 24 h, passed through a column of activated alumina under nitrogen, and stored over activated 4 Å molecular sieves prior to use. Benzene-d_6 (anhydrous, Aldrich) and tetrahydrofuran-d_8 (Cambridge Isotope Laboratories) were purified by storage over activated 4 Å molecular sieves or sodium metal prior to use. UCl_4,[39] $UI_3(THF)_4$,[40] $(C_5Me_5)_2UI(THF)$ (**3**),[41] and (PNP)H (**5**)[42] were prepared according to literature procedures.

Caution! *Depleted uranium (primary isotope ^{238}U) is a weak α-emitter (4.197 MeV) with a half-life of 4.47 × 10^9 years; manipulations and reactions should be carried out in monitored fume hoods or in an inert atmosphere drybox in a radiation laboratory equipped with α- and β-counting equipment.*

Synthesis of (PNP)K (6). A 250 mL sidearm flask equipped with a stir bar was charged with (PNP)H (**5**) (4.50 g, 10.5 mmol, 1.0 equiv), toluene (25 mL), and hexane (75 mL). To the resulting solution was added portion-wise potassium bis(trimethylsilyl)amide (3.15 g, 15.8 mmol, 1.5 equiv) at ambient temperature. The reaction mixture immediately turned orange and was stirred for 12 h, yielding a bright yellow suspension. The solid was collected by filtration through a coarse porosity frit, washed with hexane (25 mL), and thoroughly dried under reduced pressure to afford analytically pure (PNP)K (**6**) as a yellow solid (4.52 g, 9.67 mmol, 92%). ^{1}H NMR (THF-d_8, 298 K): δ 1.07 (m, 24H, CH*Me*$_2$), 2.09 (s, 6H, Ar-*Me*), 2.13 (m, 4H, C*H*Me$_2$), 6.53 (d, $^3J_{HH}$ = 8 Hz, 2H, Ar-*H*), 6.76 (s, 2H, Ar-*H*), 6.86 (dd, $^3J_{HH}$ = 8 Hz, $^4J_{PH}$ = 5 Hz, Ar-*H*). ^{13}C{^{1}H} NMR (THF-d_8, 298 K): δ 20.22 (d, J_{CP} = 11.4 Hz), 21.27 (d, J_{CP} = 9.1 Hz), 21.55 (s; Ar-*C*H$_3$), 23.14 (d, J_{CP} = 11.9 Hz), 117.3 (d, J_{CP} = 2.8 Hz), 119.5 (s), 122.5 (s), 130.5 (s), 132.8 (s), 161.4 (d, J_{CP} = 18.7 Hz). ^{31}P{^{1}H} NMR (THF-d_8, 298 K): δ −0.31 (s). Anal. Calcd for $C_{26}H_{40}KNP_2$ (mol. wt. 467.65): C, 66.78; H, 8.62; N, 3.00. Found: C, 66.49; H, 8.73; N, 2.88.

Synthesis of (PNP)UI$_2$(4-^{t}Bu-pyridine)$_2$ (7). A 50 mL sidearm flask equipped with a stir bar was charged with $UI_3(THF)_4$ (1.58 g, 1.74 mmol) and THF (10 mL). To the resulting solution was added a solution of (PNP)K (**6**) (817 mg, 1.74 mmol, 1.0 equiv) in THF (10 mL) at ambient temperature. The reaction mixture turned immediately green, was stirred for 30 min, and filtered through a Celite-padded coarse frit. The filtrate was collected, an excess of 4-^{t}Bu-pyridine (100 mg, 740 mmol) was added, and the resulting solution was stirred for 10 min. The volatiles were removed under reduced pressure, and the resulting dark green solid was washed with 10 mL of cold (−35 °C) pentane to give (PNP)UI$_2$(4-^{t}Bu-pyridine)$_2$ (**7**) as a dark green solid (2.01 g, 1.69 mmol, 97%). X-ray quality samples of **7** were obtained by recrystallization from diethyl ether at −35 °C. ^{1}H NMR (C_6D_6, 298 K): δ −24.41 (s, 6H), −13.05 (s, 6H), −3.27 (s, 6H), −1.14 (s, 2H), 2.02 (s, 2H), 2.84 (s, 4H), 4.01 (s, 18H), 4.28 (s, 6H), 4.70 (s, 6H), 5.82 (s, 2H), 14.38 (s, 4H), 19.92 (s, 2H), 44.67 (s, 2H). ^{31}P{^{1}H} NMR (C_6D_6, 298 K): no signal observed in the range ± 5000 ppm. Anal. Calcd for $C_{44}H_{66}I_2N_3P_2U$ (mol. wt. 1190.80): C, 44.38; H, 5.59; N, 3.53. Found: C, 44.79; H, 5.70; N, 3.73.

Synthesis of [(PNP)UCl$_3$]$_2$ (8). A 50 mL sidearm flask equipped with a stir bar was charged with UCl_4 (812 mg, 2.14 mmol, 1.0 equiv) and THF (10 mL). To the resulting suspension was added a solution of (PNP)K (**6**) (1.00 g, 2.14 mmol, 1.0 equiv) in THF (10 mL) at ambient temperature. The reaction mixture turned

(29) Bailey, B. C.; Fan, H.; Huffman, J. C.; Baik, M.-H.; Mindiola, D. J. *J. Am. Chem. Soc.* **2007**, *129*, 8781–8793.

(30) Masuda, J. D.; Jantunen, K. C.; Ozerov, O. V.; Noonan, K. J. T.; Gates, D. P.; Scott, B. L.; Kiplinger, J. L. *J. Am. Chem. Soc.* **2008**, *130*, 2408–2409.

(31) Arliguie, T.; Doux, M.; Mezailles, N.; Thuery, P.; Le Floch, P.; Ephritikhine, M. *Inorg. Chem.* **2006**, *45*, 9907–9913.

(32) Belkhiri, L.; Arliguie, T.; Thuery, P.; Fourmigue, M.; Boucekkine, A.; Ephritikhine, M. *Organometallics* **2006**, *25*, 2782–2795.

(33) Gaunt, A. J.; Reilly, S. D.; Enriquez, A. E.; Scott, B. L.; Ibers, J. A.; Sekar, P.; Ingram, K. I. M.; Kaltsoyannis, N.; Neu, M. P. *Inorg. Chem.* **2008**, *47*, 29–41.

(34) Gaunt, A. J.; Scott, B. L.; Neu, M. P. *Inorg. Chem.* **2006**, *45*, 7401–7407.

(35) Ingram, K. I. M.; Kaltsoyannis, N.; Gaunt, A. J.; Neu, M. P. *J. Alloys Compd.* **2007**, *444*, 369–375.

(36) Roger, M.; Belkhiri, L.; Arliguie, T.; Thuery, P.; Boucekkine, A.; Ephritikhine, M. *Organometallics* **2008**, *27*, 33–42.

(37) Brennan, J. G.; Stults, S. D.; Andersen, R. A.; Zalkin, A. *Organometallics* **1988**, *7*, 1329–1334.

(38) (a) *SAINT 7.06 Integration Software*; Bruker Analytical X-ray Systems: Madison, WI, 2003. (b) Sheldrick, G. M. *SADABS 2.03 Program for Adsorption Correction*; University of Göttingen: Göttingen, Germany, 2001. (c) Sheldrick, G. M. *SHELXTL 5.10, Structure Solution and Refinement Package*; University of Göttingen: Göttingen, Germany, 1997.

(39) Kiplinger, J. L.; Morris, D. E.; Scott, B. L.; Burns, C. J. *Organometallics* **2002**, *21*, 5978–5982.

(40) Avens, L. R.; Bott, S. G.; Clark, D. L.; Sattelberger, A. P.; Watkin, J. G.; Zwick, B. D. *Inorg. Chem.* **1994**, 2248–2256.

(41) Avens, L. R.; Burns, C. J.; Butcher, R. J.; Clark, D. L.; Gordon, J. C.; Schake, A. R.; Scott, B. L.; Watkin, J. G.; Zwick, B. D. *Organometallics* **2000**, *19*, 451–457.

(42) Fan, L.; Foxman, B. M.; Ozerov, O. V. *Organometallics* **2004**, *23*, 326–328.

immediately red, was stirred for 30 min, and filtered through a Celite-padded coarse frit. The filtrate was collected, and the volatiles were removed under reduced pressure to give $[(PNP)UCl_3]_2$ (**8**) as a red solid (1.62 g, 1.05 mmol, 98%). ^{1}H NMR (C_6D_6, 298 K): δ −26.40 (s, 6H), −19.99 (s, 6H), −9.66 (s, 2H), −8.53 (s, 6H), −1.47 (s, 2H), 1.09 (s, 6H), 4.40 (s, 2H), 6.91 (s, 6H), 21.45 (s, 2H), 43.57 (s, 2H). ^{31}P{^{1}H} NMR (C_6D_6, 298 K): δ 1157.3 (br s). Anal. Calcd for $C_{52}H_{80}Cl_6N_2P_4U_2$ (mol. wt. 1542.44): C, 40.40; H, 5.22; N, 1.81. Found: C, 40.39; H, 5.62; N, 2.0.

Characterization of (PNP)UCl$_3$(THF) (9). Complex **9** is formed in equilibrium with **8** (52/48 ratio at 25 °C in THF-d_8) upon dissolution of **8** in THF. Crystals of **9** were obtained by cooling a concentrated solution of **8** in THF at −35 °C. Upon drying under reduced pressure, crystals of **9** resort to pure **8**. ^{1}H NMR (THF-d_8, 298 K): δ −23.62 (s, 6H), −19.20 (s, 6H), −9.35 (s, 2H), −6.77 (s, 6H), −6.16 (s, 2H), −3.21 (s, 2H), 0.16 (s, 6H), 5.54 (s, 6H), 19.03 (s, 2H), 38.04 (s, 2H). ^{31}P{^{1}H} NMR (THF-d_8, 298 K): δ 1151.2 (s).

Synthesis of (PNP)UCl$_3$(TMPO)$_2$ (10). A 50 mL sidearm flask equipped with a stir bar was charged with UCl_4 (812 mg, 2.14 mmol, 1.0 equiv) and THF (10 mL). To the resulting suspension was added a solution of (PNP)K (**6**) (1.00 g, 2.14 mmol, 1.0 equiv) in THF (10 mL) at ambient temperature. The reaction mixture turned immediately red, was stirred for 30 min, and filtered through a Celite-padded coarse frit. The filtrate was collected, trimethylphosphine oxide (TMPO, 394 mg, 4.28 mmol, 2.0 equiv) was added as a solid, and the resulting solution was stirred for 10 min. The volatiles were removed under reduced pressure to give $(PNP)UCl_3(TMPO)_2$ (**10**) as a red solid (2.01 g, 2.10 mmol, 98%). X-ray quality samples of **10** were obtained by recrystallization from THF and TMS_2O at −35 °C. ^{1}H NMR (THF-d_8, 323 K): δ −19.75 (s, 6H), −17.29 (s, 6H), −10.63 (s, 2H), −7.15 (s, 2H), −5.04 (s, 6H), −0.14 (s, 6H), 2.94 (s, 2H), 4.86 (s, 6H), 13.62 (s, 18H, *Me*$_3$P=O), 17.63 (s, 2H), 34.80 (s, 2H). ^{31}P{^{1}H} NMR (THF-d_8, 323 K): δ 80.5 (s, Me$_3$P=O), 1057.9 (br s, PNP). ^{1}H NMR (THF-d_8, 223 K): δ −43.29 (s, 3H), −37.78 (s, 3H), −29.59 (s, 3H), −25.99 (s, 3H), −24.27 (s, 1H), −19.57 (s, 1H), −17.87 (s, 1H), −10.97 (s, 1H), −10.25 (s, 3H), −8.01 (s, 1H), −6.41 (s, 1H), 0.15 (s, 3H), 2.29 (s, 9H, *Me*$_3$P=O), 2.85 (s, 3H), 6.88 (s, 3H), 7.13 (s, 3H), 17.15 (s, 1H), 19.94 (s, 3H), 26.68 (s, 1H), 33.12 (s, 9H, *Me*$_3$P=O), 34.15 (s, 1H), 57.49 (s, 1H). ^{31}P{^{1}H} NMR (THF-d_8, 223 K): δ 85.3 (s, Me$_3$P=O), 157.4 (s, Me$_3$P=O), 1277.9 (br s, PNP). Anal. Calcd for $C_{32}H_{58}Cl_3NO_2P_4U$ (mol. wt. 957.09): C, 40.16; H, 6.11; N, 1.46. Found: C, 40.21; H, 5.97; N, 1.31.

Synthesis of (PNP)UCl$_3$(TPPO) (11). A 50 mL sidearm flask equipped with a stir bar was charged with UCl_4 (812 mg, 2.14 mmol, 1.0 equiv) and THF (10 mL). To the resulting suspension was added a solution of (PNP)K (**6**) (1.00 g, 2.14 mmol, 1.0 equiv) in THF (10 mL) at ambient temperature. The reaction mixture turned immediately red, was stirred for 30 min, and filtered through a Celite-padded coarse frit. The filtrate was collected, triphenylphosphine oxide (TPPO, 595 mg, 2.14 mmol, 1.0 equiv) was added as a solid, and the resulting solution was stirred for 10 min. The volatiles were removed under reduced pressure, and the resulting red solid was washed with 10 mL of pentane to give $(PNP)UCl_3(TPPO)$ (**11**) as a red solid (2.21 g, 2.10 mmol, 98%). ^{1}H NMR (C_6D_6, 298 K): δ −23.72 (s, 6H), −20.42 (s, 6H), −13.04 (s, 2H), −8.17 (s, 2H), −6.59 (s, 6H), −1.57 (s, 6H), 4.79 (s, 2H), 6.58 (s, 6H), 9.47 (s, 3H), 10.07 (s, 6H), 21.30 (s, 2H), 23.82 (s, 6H), 44.89 (s, 2H). ^{31}P{^{1}H} NMR (C_6D_6, 298 K): δ 127.4 (s, Ph_3P=O), 1160.1 (br s, PNP). Anal. Calcd for $C_{44}H_{55}Cl_3NOP_3U$ (mol. wt. 1051.22): C, 50.27; H, 5.27; N, 1.33. Found: C, 49.96; H, 5.31; N, 1.30.

Synthesis of (PNP)$_2$UI (12). A 50 mL sidearm flask equipped with a stir bar was charged with $UI_3(THF)_4$ (930 mg, 1.03 mmol, 1.0 equiv) and THF (10 mL). To the resulting mixture was added a solution of (PNP)K (**6**) (963 mg, 2.06 mmol, 2.0 equiv) in THF (10 mL) at ambient temperature. The reaction mixture turned immediately green, was stirred for 2 days, and filtered through a Celite-padded coarse frit. The filtrate was collected, the volatiles were removed under reduced pressure, and the resulting dark green solid was washed with 10 mL of cold (−35 °C) hexane to give $(PNP)_2UI$ (**13**) as a dark green solid (1.22 g, 1.00 mmol, 97%). X-ray quality samples of **13** were obtained by recrystallization from hexane at −35 °C. ^{1}H NMR (THF-d_8, 273 K): δ −39.92(s, 1H), −32.96 (s, 1H), −31.53 (s, 3H), −28.45 (s, 6H), −25.21 (s, 3H), −22.70 (s, 3H), −21.05 (s, 1H), −16.16 (s, 6H), −13.17 (s, 3H), −9.27 (s, 1H), −6.34 (s, 3H), −5.94 (s, 3H), −5.66 (s, 3H), −2.30 (s, 3H), −1.73 (s, 6H), 3.04 (s, 3H), 5.63 (s, 1H), 6.29 (s, 1H), 6.47 (s, 1H), 8.11 (s, 6H), 10.13 (s, 3H), 10.88 (s, 1H), 11.11 (s, 1H), 11.34 (s, 3H), 13.73 (s, 1H), 14.07 (s, 1H), 15.67 (s, 1H), 16.85 (s, 1H), 18.88 (s, 1H) 26.85 (s, 1H), 30.38 (s, 3H), 34.14 (s, 1H), 38.75 (s, 1H), 56.41 (s, 1H), 68.12 (s, 1H), 96.80 (s, 1H). ^{31}P{^{1}H} NMR (THF-d_8, 298 K): no signal observed in the range ±5000 ppm. Anal. Calcd for $C_{52}H_{80}IN_2P_4U$ (mol. wt. 1222.03): C, 51.11; H, 6.60; N, 2.29. Found: C, 50.80; H, 6.84; N, 2.15.

Synthesis of (PNP)$_2$UCl$_2$ (13). A 50 mL sidearm flask equipped with a stir bar was charged with UCl_4 (391 mg, 1.03 mmol, 1.0 equiv) and THF (10 mL). To the resulting suspension was added a solution of (PNP)K (**6**) (963 mg, 2.06 mmol, 2.0 equiv) in THF (10 mL) at ambient temperature. The reaction mixture turned immediately red, was stirred for 2 days, and then concentrated to 10 mL. Pentane (10 mL) was added, and the solution was filtered through a Celite-padded coarse frit. The filtrate was collected, and volatiles were removed under reduced pressure to give $(PNP)_2UCl_2$ (**12**) as a red solid (1.19 g, 1.02 mmol, 99%). X-ray quality samples of **12** were obtained by recrystallization from a mixture of THF and TMS_2O at −35 °C. ^{1}H NMR (THF-d_8, 323 K): δ −35.43 (s, 6H), −21.34 (s, 6H), −19.99 (s, 2H), −7.68 (s, 2H), −4.83 (s, 2H), −2.48 (s, 6H), 4.68 (s, 6H), 5.70 (s, 6H), 6.61 (s, 12H), 7.83 (s, 6H), 9.03 (s, 2H), 9.24 (s, 6H), 10.36 (s, 2H), 11.69 (s, 6H), 13.33 (s, 2H), 14.80 (s, 2H), 17.15 (s, 2H), 41.21 (s, 2H), 49.46 (s, 2H). ^{31}P{^{1}H} NMR (THF-d_8, 323 K): δ 56.1 (s), 1469.3 (s). ^{1}H NMR (THF-d_8, 223 K): δ −57.79 (s, 6H), −54.15 (s, 2H), −51.31 (s, 6H), −40.12 (s, 2H), −29.54 (s, 6H), −22.81 (s, 2H), −17.74 (s, 6H), −15.12 (s, 6H), −3.49 (s, 6H), −2.88 (s, 6H), 2.19 (s, 2H), 6.57 (s, 6H), 13.81 (s, 2H), 17.24 (s, 6H), 25.20 (s, 2H), 42.91 (s, 6H), 45.90 (s, 2H), 60.66 (s, 2H), 108.43 (s, 2H), 141.20 (s, 2H). ^{31}P{^{1}H} NMR (THF-d_8, 223 K): δ 50.3 (s), 1401.1 (s). Anal. Calcd for $C_{52}H_{80}IN_2P_4U$ (mol. wt. 1166.03): C, 53.26; H, 6.92; N, 2.40. Found: C, 53.23; H, 7.04; N, 2.29.

Results and Discussion

Synthesis of Mono(PNP) Uranium(III)/(IV) Complexes. A major reason for the success of the pentamethylcyclopentadienyl ligand in organometallic uranium chemistry is due to its ability to stabilize uranium in a wide range (III, IV, V, and VI) of oxidation states.[15] This entire body of chemistry relies on the low-valent uranium(III) and uranium(IV) halide complexes as starting materials shown in Chart 2, namely, the mono(C_5Me_5) complexes **1**−**2** and the bis(C_5Me_5) complexes **3**−**4**. To develop a new and versatile platform

Table 1. Crystallographic Experimental Parameters for **7**, **9**, **10**·2 THF, **12**·*n*-hexane, and **13**·THF

	7	**9**	**10**·2 THF	**12**·*n*-hexane	**13**·THF
formula	$C_{44}H_{66}I_2N_3P_2U$	$C_{38}H_{64}Cl_3NO_3P_2U$	$C_{40}H_{74}Cl_3NO_4P_4U$	$C_{64}H_{108}IN_2P_4U$	$C_{56}H_{88}Cl_2N_2OP_4U$
a (Å)	14.174(3)	11.9601(14)	15.3705(12)	19.211(4)	13.6641(18)
b (Å)	14.912(3)	14.2707(17)	20.0629(15)	23.405(5)	14.1260(18)
c (Å)	23.424(5)	24.803(3)	15.7578(12)	23.373(6)	17.874(2)
α (deg)	90	90	90	90	91.607(1)
β (deg)	102.151(2)	90	93.0930(10)	90	110.087(1)
γ (deg)	90	90	90	90	113.515(1)
V (Å^3)	4839.9(18)	4233.3(9)	4852.3(6)	12758(5)	2916.0(7)
Z	4	4	4	8	2
fw	1190.77	989.22	1101.26	1394.33	1238.09
space group	$P2_1/n$	$P2_12_12_1$	$P2_1/n$	*Pbca*	$P\bar{1}$
T (K)	120(1)	120(1)	120(1)	120(1)	120(1)
λ (Å)	0.71073	0.71073	0.71073	0.71073	0.71073
D_{calcd} (g cm^{-3})	1.634	1.552	1.507	1.452	1.410
μ (mm^{-1})	4.726	4.134	3.679	3.168	3.022
R1 [$I > 2\sigma(I)$]	0.0347	0.0441	0.0312	0.0486	0.0406
wR2 (all data)	0.0862	0.0978	0.0736	0.1070	0.1090

Scheme 1. Synthesis of (PNP)K (**6**) and the Mono(PNP) Uranium(III) Complex **7**

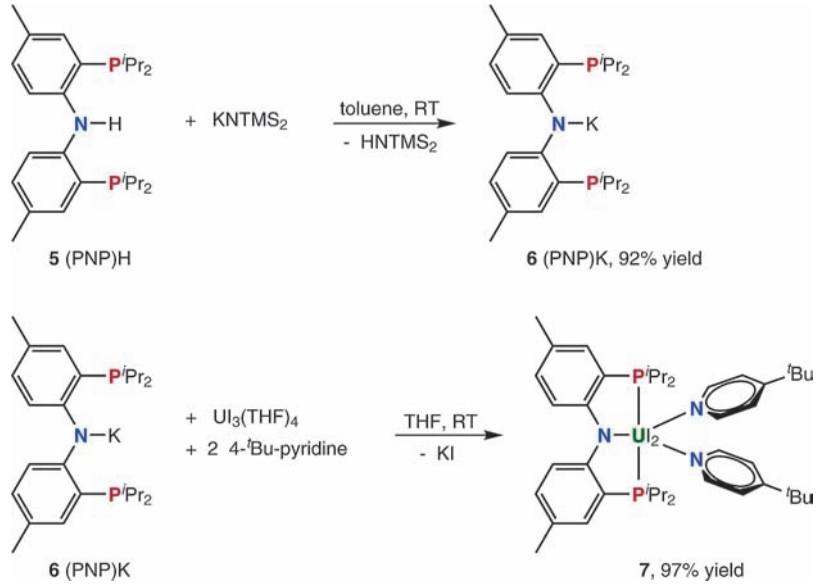

for uranium chemistry based on the PNP ligand framework, similar mono(PNP) and bis(PNP) uranium(III) and uranium(IV) halide complexes were prepared and characterized.

Entry into the low-valent uranium(III) mono(PNP) system is illustrated in Scheme 1. Using K[N(SiMe$_3$)$_2$] in THF solution, the ligand (PNP)H (**5**) was deprotonated to give the corresponding potassium compound, (PNP)K (**6**) in 92% isolated yield. Subsequent addition of 1 equiv of (PNP)K (**6**) to a solution of $UI_3(THF)_4$ in THF resulted in a rapid color change from deep blue to dark green accompanied by the formation of KI as an off-white precipitate. The $^{31}P\{^1H\}$ NMR spectrum of the crude mixture was uninformative as no signal could be observed in the range ±5000 ppm.[43] Although the ^1H NMR spectrum showed broad resonances confirming the coordination of the PNP ligand to an uranium(III) metal center, the structure of the complex could not be unambiguously determined from these data. Crystalline material suitable for X-ray diffraction analysis was obtained by carrying out the same reaction in the presence of an excess of 4-tert-butylpyridine from which complex **7** could be isolated as an analytically pure solid in an excellent 97% yield. The ^1H NMR spectrum of **7** in benzene-d_6 reveals that the coordination of two 4-tert-butylpyridine ligands is maintained in solution. The signals for the PNP ligand protons are all paramagnetically shifted and feature an integration pattern consistent with overall C_s or C_2 symmetry.

Complex **7** represents the first example of a PNP complex in the actinide series; the molecular structure confirms the coordination of the PNP ligand to the uranium(III) metal

Chart 2

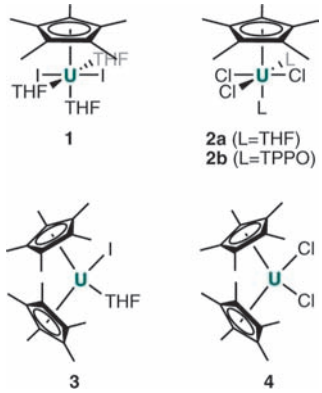

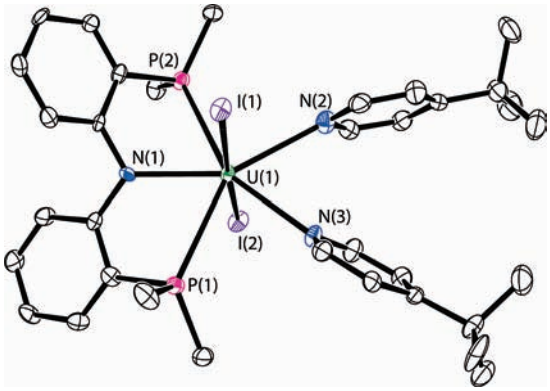

Figure 1. Molecular structure of complex **7** with thermal ellipsoids projected at the 50% probability level. Hydrogen atoms and methyl groups on the PNP ligand have been omitted for clarity. Selected bond distances (Å) and angles (deg): U(1)−N(1) 2.417(4), U(1)−N(2) 2.731(5), U(1)−N(3) 2.628(4), U(1)−P(1) 3.029(1), U(1)−P(2) 3.009(1), U(1)−I(1) 3.106(1), U(1)−I(2) 3.116(1), P(1)−U(1)−N(1) 66.16(11), P(2)−U(1)−N(1) 66.43(11), I(1)−U(1)−I(2) 175.19(1), N(2)−U(1)−N(3) 68.85(14).

center, the coordination sphere of the metal ion being completed by two iodide and two 4-tert-butylpyridine ligands (Figure 1).[44] The PNP ligand coordinates to the uranium metal center in a regular κ^3-(*P*,*N*,*P*) mode, with the metal center being roughly located in the plane of the three P, N, and P donor atoms (δ_{PUNP} = 167.9°). This is in agreement with known complexes in transition metal and lanthanide series featuring this PNP ligand.[24,30,42,45,46] Because of the large ionic radius of uranium (U^{III} 1.18 Å, U^{IV} 1.05 Å),[47] the metal center is unable to fit within the P−N−P chelate. As a consequence, the phosphine donors are pulled back and the P(1)−U(1)−P(2) angle (131.16(4)°) is far smaller than the usual 165−170° typically seen for late transition metals. At 3.02 Å, the average U−P bond distance lies at the low end of the range for other structurally characterized uranium(III) phosphine complexes,[48] whereas the U−N_{amide} bond distance (2.417(4) Å) lies at the high end of the range of known uranium(III) amide complexes.[49] This is likely a consequence of the κ^3-(*P*,*N*,*P*) coordination mode, which strengthens the U−P interactions while delocalizing the nitrogen lone pair over the two phenyl rings leading to a longer U−N_{amide} bond.[50] It is important to also note that unlike many ligand frameworks,[51−59] the PNP ligand avoids formation of an "ate complex" in **7** as well as in the other uranium complexes presented herein.

The uranium(IV) mono(PNP) complexes are also easily accessed. As shown in Scheme 2, addition of 1 equiv of (PNP)K (**6**) to UCl_4 in THF solution leads to the immediate formation of complex **8**, which was isolated in 98% after removal of the KCl byproduct and drying. The ^{1}H NMR spectrum for **8** also reflects C_s or C_2 symmetry in solution with paramagnetically shifted signals. The ^{31}P{^{1}H} NMR spectrum consists of a broad singlet at δ 1157.3 ppm indicating a κ^3-(*P*,*N*,*P*) coordinated PNP ligand. Though no crystals suitable for X-ray diffraction analysis could be obtained for **8**, it is likely that this compound exists as a dimer, with chlorine bridging atoms, considering the coordinative unsaturation of the (PNP)UCl_3 unit.[60] In fact, attempts to crystallize **8** from a THF solution afforded **9**, which was subjected to scrutiny by X-ray diffraction analysis (Figure 2). The U−P and U−N bond lengths measured in **9** are in agreement with known uranium(IV) phosphine[61] and amide complexes (Table 2).[62] The THF ligand in **9** was found to be labile and drying crystals of **9** under reduced pressure allowed full recovery of complex **8**. Moreover, dissolution of **8** in THF-d_8 yields an equilibrium mixture of the two complexes **8**:**9** (48:52 ratio), which allowed for full characterization of **9** by ^{1}H and ^{31}P{1H} NMR spectroscopy.

(43) The ^{31}P NMR spectra of uranium(III) phosphine complexes are usually silent because of an extreme broadening of the signals associated with a large paramagnetic shift. For example, see: Gradoz, P.; Ephritikhine, M.; Lance, M.; Vigner, D.; Nierlich, M. *J. Organomet. Chem.* **1994**, *481*, 69–73.

(44) The coordination chemistry of another type of bis-phosphine-amide ligand to uranium(IV) and thorium(IV) has been studied in the past; namely, the bis[2-(diisopropylphosphino)ethyl]- and bis[2-(diethylphosphino)ethyl]amides. These ligands provided highly fluxional structures (with κ^1-(*N*), κ^2-(*P*,*N*) and κ^3-(*P*,*N*,*P*) coordination modes) because of the flexible ethyl fragment in the P-N linkage. see: Coles, S. J.; Danopoulos, A. A.; Edwards, P. G.; Hursthouse, M. B.; Read, P. W. *J. Chem. Soc., Dalton Trans.* **1995**, 3401–3408.

(45) Gatard, S.; Celenligil-Cetin, R.; Guo, C. Y.; Foxman, B. M.; Ozerov, O. V. *J. Am. Chem. Soc.* **2006**, *128*, 2808–2809.

(46) Weng, W.; Guo, C. Y.; Celenligil-Cetin, R.; Foxman, B. M.; Ozerov, O. V. *Chem. Commun.* **2006**, 197–199.

(47) Shannon, R. D. *Acta Crystallogr., Sect. A* **1976**, *32*, 751–767.

(48) A Cambridge Structural Database search afforded four uranium(III) phosphine structures with an average U−P bond length of 3.051 Å (range 0.241 Å). For specific references, see: (a) $(C_5Me_5)_2UH(DMPE)$, U−P = 3.211(8), 3.092(8) Å:Duttera, M. R.; Fagan, P. J.; Marks, T. J.; Day, V. W. *J. Am. Chem. Soc.* **1982**, *104*, 865–867. (b) $(MeC_5H_4)_3U(PMe_3)$, U−P = 2.972(6) Å:Brennan, J. G.; Zalkin, A. *Acta Crystallogr.* **1985**, *41C*, 1038–1040. (c) $(C_5H_5)_3U(Me_2P\text{-}CH_2\text{-}CH_2\text{-}PMe_2)U(C_5H_5)_3$, U−P = 3.020(6), 3.024(6) Å:Zalkin, A.; Brennan, J. G.; Andersen, R. A. *Acta Crystallogr.* **1987**, *43C*, 1706–1708. (d) $(MeC_5H_4)_3U[P(OCH_2)_3CEt]$, U−P = 2.988(6) Å:Brennan, J. G.; Stults, S. D.; Andersen, R. A.; Zalkin, A. *Organometallics* **1988**, *7*, 1329–1334.

(49) A Cambridge Structural Database search afforded twelve uranium(III) amide structures with an average U−N bond length of 2.381 Å (range 0.470 Å). For representative examples of complexes possessing an U−N_{amide} linkage, see: (a) $\{U[N(SiMe_3)_2]_4\}\{K(THF)_6\}$, U−N = 2.431(6), 2.430(6), 2.430(7), 2.439(6) Å:Evans, W. J.; Lee, D. S.; Rego, D. B.; Perotti, J. M.; Kozimor, S. A.; Moore, E. K.; Ziller, J. W. *J. Am. Chem. Soc.* **2004**, *126*, 14574–14582. (b) $(C_5Me_5)_2U[N(SiMe_3)_2]$, U−N = 2.352(2) Å:Evans, W. J.; Nyce, G. W.; Forrestal, K. J.; Ziller, J. W. *Organometallics* **2002**, *21*, 1050–1055. (c) $[(Me_3Si)_2N]_4U_2[\mu\text{-}N(H)(2,4,6\text{-}Me_3\text{-}C_6H_2)]_2$, U−N = 2.354, 2.324 Å:Stewart, J. L.; Andersen, R. A. *New J. Chem.* **1995**, *19*, 587–595.

(50) The U−N_{amide} bond distance of 2.489(9) Å reported for the uranium(III) bis(arylamide) complex $(Tp^{Me2})_2U[N(C_6H_5)_2]$ is long:Antunes, M. A.; Ferrence, G. M.; Domingos, A.; McDonald, R.; Burns, C. J.; Takats, J.; Marques, N. *Inorg. Chem.* **2004**, *43*, 6640–6643.

(51) Arney, D. S. J.; Burns, C. J. *J. Am. Chem. Soc.* **1995**, *117*, 9448–9460.

(52) Blake, P. C.; Hey, E.; Lappert, M. F.; Atwood, J. L.; Zhang, H. M. *J. Organomet. Chem.* **1988**, *353*, 307–314.

(53) Blake, P. C.; Lappert, M. F.; Atwood, J. L.; Zhang, H. M. *J. Chem. Soc., Chem. Commun.* **1988**, 1436–1438.

(54) Edelman, M. A.; Lappert, M. F. *Inorg. Chim. Acta* **1987**, *139*, 185–186.

(55) Jantunen, K. C.; Haftbaradaran, F.; Katz, M. J.; Batchelor, R. J.; Schatte, G.; Leznoff, D. B. *Dalton Trans.* **2005**, 3083–3091.

(56) Korobkov, I.; Gambarotta, S.; Yap, G. P. A.; Thompson, L.; Hay, P. J. *Organometallics* **2001**, *20*, 5440–5445.

(57) Schnabel, R. C.; Scott, B. L.; Smith, W. H.; Burns, C. J. *J. Organomet. Chem.* **1999**, *591*, 14–23.

(58) Secaur, C. A.; Day, V. W.; Ernst, R. D.; Kennelly, W. J.; Marks, T. J. *J. Am. Chem. Soc.* **1976**, *98*, 3713–3715.

(59) Villiers, C.; Thuery, P.; Ephritikhine, M. *Chem. Commun.* **2007**, 2832–2834.

(60) The absence of any coordinated solvent or the formation of any "ate complex" was verified by ^{1}H NMR spectroscopy and C,H,N elemental analyses.

Scheme 2. Synthesis of the Mono(PNP) Uranium(IV) Complexes **8**−**11**

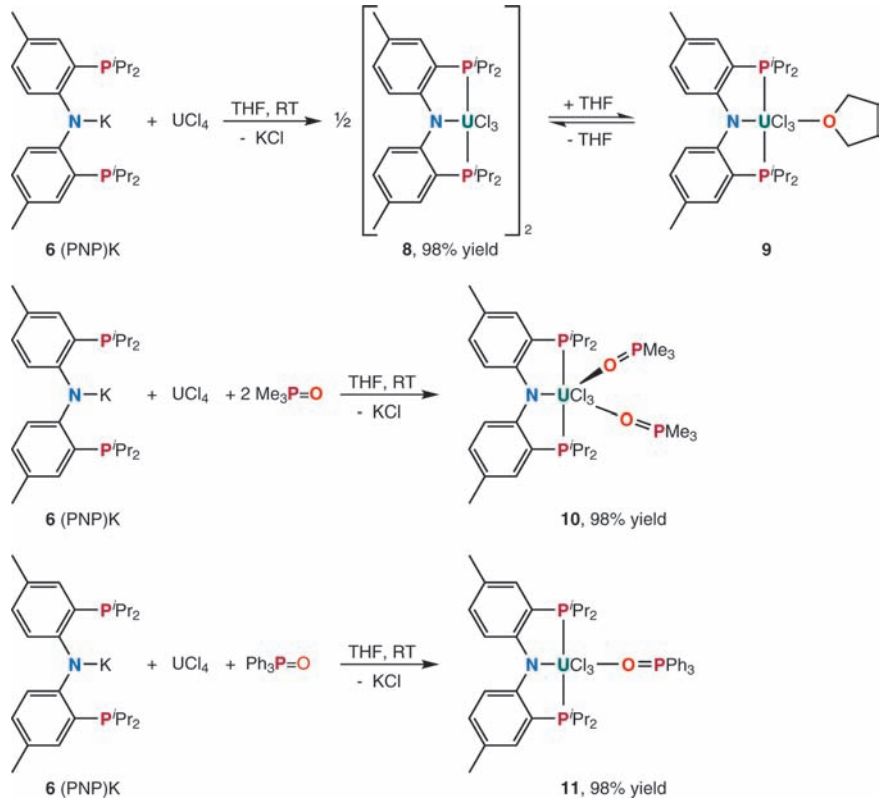

Table 2. Selected Metrical Parameters for the (PNP)-Uranium Complexes **7**, **9**, **10**, **12**, and **13**

complex	U−N (Å)		U−P (Å)			U−X (Å)			torsion angle δ(PUPN)	
7 (X = I)	2.417(4)		3.009(1)		3.019(1)	3.106(1)		3.116(1)	167.9°	
9 (X = Cl)	2.343(7)		2.962(2)		3.041(2)	2.597(2)	2.642(2)	2.610(2)	160.5°	
10 (X = Cl)	2.411(3)		2.989(1)		3.116(1)	2.726(1)	2.745(1)	2.687(1)	155.9°	
12 (X = I)	2.376(5)	2.439(5)	3.063(2)	3.076(2)	3.197(2) 3.316(2)		3.109(1)		176.2°	128.3°
13 (X = Cl)	2.279(3)	2.290(3)	2.996(1)		3.004(1)	2.576(1)		2.590(1)	78.5°	89.3°

Phosphine oxides proved to be excellent reagents for cleaving the dimer complex **8** to form well-defined mono(PNP) uranium(IV) complexes. Indeed, addition of 2 equiv of trimethylphosphine oxide (TMPO) yields the mono(PNP) complex **10**, in which the metal ion is stabilized by two TMPO ligands (Scheme 2). Complex **10** was characterized using ^{1}H and ^{31}P{^{1}H} NMR spectroscopy, elemental analysis, and solid-state X-ray crystallography. As seen in Table 2, the metrical parameters for **10** hardly differ from those of **9**. The molecular structure of complex **10** is presented in Figure 3and reveals that the TMPO ligands are located in different coordination sites that can be described as pseudoapical (defined by O(2)) and pseudoaxial (defined by O(1)) positions, with respect to the PNP ligand. The ^{1}H and ^{31}P{^{1}H} spectra of **10** in THF-d_8 at ambient temperature show unusually broad resonances, which suggests fluxional behavior on the NMR time scale. Variable temperature NMR studies were performed to determine if this behavior was due to dissociation of a TMPO ligand or the fast exchange of the TMPO ligands between the two different coordination sites. At −50 °C, the ^{31}P{^{1}H} NMR spectrum of **10** shows three singlets at δ 1277.9, 157.4, and 85.3 ppm. The ^{1}H NMR spectrum directly derives from that of complex **9** but shows two additional signals at δ 33.12 and 2.29 ppm for the methyl groups of the TMPO ligands. In total, these data point to a rigid structure as shown by X-ray crystallography where the PNP ligand adopts a κ^3-(*P*,*N*,*P*) coordination mode, and the two TMPO ligands are in different coordination sites. At high temperature (+50 °C), the resonances for the TMPO

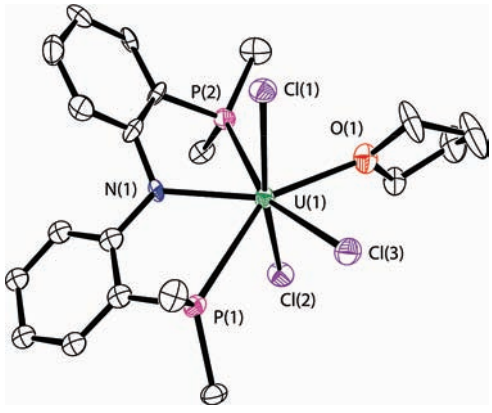

Figure 2. Molecular structure of complex **9** with thermal ellipsoids projected at the 50% probability level. Hydrogen atoms and methyl groups have been omitted for clarity. Selected bond distances (Å) and angles (deg): U(1)−N(1) 2.343(7), U(1)−O(1) 2.485(6), U(1)−P(1) 2.962(2), U(1)−P(2) 3.041(2), U(1)−Cl(1) 2.610(2), U(1)−Cl(2) 2.597(2), U(1)−Cl(3) 2.642(2), P(1)−U(1)−N(1) 66.99(17), P(2)−U(1)−N(1) 66.33(17), Cl(1)−U(1)−Cl(2) 163.21(7), O(1)−U(1)−Cl(3) 78.22(16).

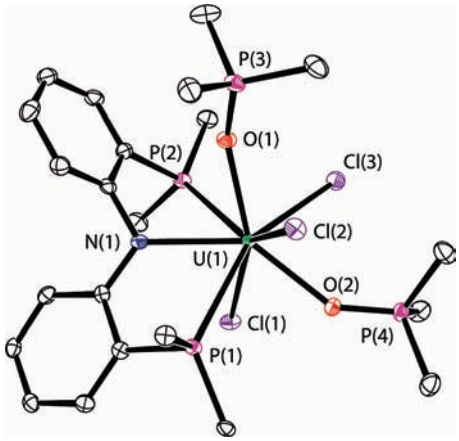

Figure 3. Molecular structure of complex **10** with thermal ellipsoids projected at the 50% probability level. Hydrogen atoms and methyl groups on the PNP ligand have been omitted for clarity. Selected bond distances (Å) and angles (deg): U(1)−N(1) 2.411(2), U(1)−O(1) 2.341(2), U(1)−O(2) 2.343(2), U(1)−P(1) 2.989(1), U(1)−P(2) 3.116(1), U(1)−Cl(1) 2.687(1), U(1)−Cl(2) 2.745(1), U(1)−Cl(3) 2.726(1), P(1)−U(1)−N(1) 64.78(7), P(2)−U(1)−N(1) 62.61(7), Cl(1)−U(1)−Cl(2) 140.54(3), Cl(1)−U(1)−Cl(3) 97.59(3), Cl(2)−U(1)−Cl(3) 98.47(3), O(1)−U(1)−O(2) 78.22(16).

ligands collapse into a singlet at δ 80.5 ppm, whereas the signal for the two coordinated phosphines are found at δ 1057.9 ppm. The ^{1}H NMR spectrum shows a unique resonance δ 13.62 ppm for the 18 protons of the TMPO ligands. No free TMPO is observed in either the ^{31}P{^{1}H} or ^{1}H spectra ruling out any dissociation processes.

The addition of excess triphenylphosphine oxide (TPPO) to a THF solution of **8** similarly yields the monomeric uranium(IV) complex **11** (in 98% isolated yield), in which only one phosphine oxide is coordinated to the metal center. No exchange with free TPPO is observed by NMR. Complexes **9** and **11** are the mono(PNP) analogues of the mono(C_5Me_5) complexes **2a** and **2b**, respectively. However, two ligands (THF or TPPO) are required to stabilize the (C_5Me_5)UCl_3 moiety in **2a** and **2b**, but only one can bind to the metal center in **9** and **11**. Since two neutral donors are able to coordinate to the metal center of the (PNP)UCl_3 fragment (see **10**), this indicates that a more sterically congested environment is provided by the PNP ligand.

It is interesting to note that the syntheses of the mono(C_5Me_5) complexes **1** and **2** were originally developed to access sterically and electronically unsaturated uranium centers with enhanced reactivities compared to the bis(C_5Me_5) systems. However, this strategy did not meet with the expected success as the electronically unsaturated metal center coupled with the presence of extra available coordination sites results in unwanted reactions with solvent molecules.[63] In fact, most of the mono(C_5Me_5) complexes reported to date were obtained from reactions of bis(C_5Me_5) precursors. From this perspective, the PNP ligand set shows great promise for expanding the chemistry of uranium supported by a single anionic ligand.

Synthesis of Bis(PNP) Uranium(III)/(IV) Complexes. Considering the extensive body of work developed with the (C_5Me_5)$_2$U framework using (C_5Me_5)$_2$UI(THF) (**3**) and (C_5Me_5)$_2UCl_2$ (**4**), it was of interest to access the isostructural complexes with the PNP ligand. Despite the steric hindrance of the PNP ligand, reaction of 2 equiv of (PNP)K (**6**) with $UI_3(THF)_4$ in THF solution for 2 days at room temperature gave the bis(PNP) uranium iodide complex **12**, which was isolated in 97% isolated yield after workup (Scheme 3). This complex represents the first example of the coordination of two PNP ligands on the same metal center. The ^{1}H NMR spectrum of **12** reveals a dynamic process at room temperature; however, at 0 °C it shows the coordination of two PNP ligands with an overall C_1 symmetry, which is lower than observed for complexes **7**−**11**. Given that even at −50 °C the κ^3-(*P*,*N*,*P*)-coordinated PNP ligand presents a local C_s or C_2 symmetry (see **10**), we propose that the reduction

Scheme 3. Synthesis of Bis(PNP) Uranium(III) Complex **12** and Uranium(IV) Complex **13**

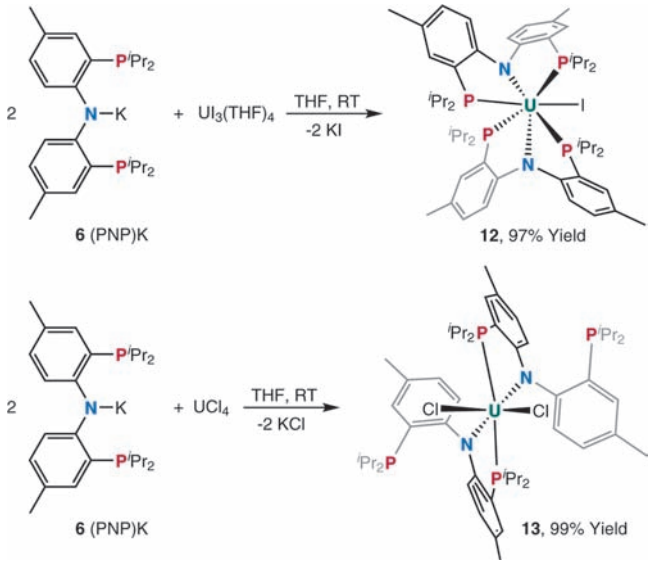

(61) A Cambridge Structural Database search afforded five uranium(IV) phosphine structures with an average U−P bond length of 3.063 Å (range 0.205 Å). For specific references, see: (a) $U(OC_6H_5)_4(DMPE)_2$, U−P = 3.102(6), 3.116(6), 3.105(6), 3.097(6) Å:Edwards, P. G.; Andersen, R. A.; Zalkin, A. *J. Am. Chem. Soc.* **1981**, *103*, 7792–7794. (b) $U(CH_3)(CH_2C_6H_5)_3$(DMPE), U−P = 3.020(5), 3.010(2) Å:Edwards, P. G.; Andersen, R. A.; Zalkin, A. *Organometallics* **1984**, *3*, 293–298. (c) $U(BH_3Me)_4$(DMPE), U−P = 3.029(2), 3.017(2) Å:Brennan, J.; Shinomoto, R.; Zalkin, A.; Edelstein, N. *Inorg. Chem.* **1984**, *23*, 4143–4146. (d) U{κ^2-(*P*,*P*)-[$P(CH_2CH_2PMe_2)_2$]}$_4$, U−P = 3.109(2), 2.988(2), 2.976(2), 2.980(2) Å:Edwards, P. G.; Parry, J. S.; Read, P. W. *Organometallics* **1995**, *14*, 3649–3658. (e) UCl_2{κ^3-(*P*,*N*)-[$N(CH_2CH_2PEt_2)_2$]}$_2$, U−P = 3.103(1), 3.155(1), 3.115(1), 3.181(1), 3.085(1), 3.097(1) Å:Coles, S. J.; Danopoulos, A. A.; Edwards, P. G.; Hursthouse, M. B.; Read, P. W. *J. Chem. Soc., Dalton Trans.* **1995**, 3401–3408.

(62) A Cambridge Structural Database search afforded 46 uranium(IV) amide structures with an average U−N bond length of 2.245 Å (range 0.351 Å). For representative examples of complexes containing a $U-N_{amide}$ linkage, see: (a) $Cp_3U[N(C_6H_5)_2]$, U−N = 2.29(1) Å:Cramer, R. E.; Engelhardt, U.; Higa, K. T.; Gilje, J. W. *Organometallics* **1987**, *6*, 41–45. (b) $(C_5Me_5)_2U[NH(2,6\text{-}Me_2\text{-}C_6H_3)]_2$, U−N = 2.267(6) Å:Straub, T.; Frank, W.; Reiss, G. J.; Eisen, M. S. *J. Chem. Soc., Dalton Trans.* **1996**, 2541–2546. (c) [$Me_2Si(h^5\text{-}C_5Me_4)(^t$BuN)]U$(NMe_2)_2$, U−N = 2.278(4), 2.207(4), 2.212(4) Å:Stubbert, B. D.; Stern, C. L.; Marks, T. J. *Organometallics* **2003**, *22*, 4836–4838.

(63) Larch, C. P.; Cloke, F. G. N.; Hitchcock, P. B. *Chem. Commun.* **2008**, 82–84.

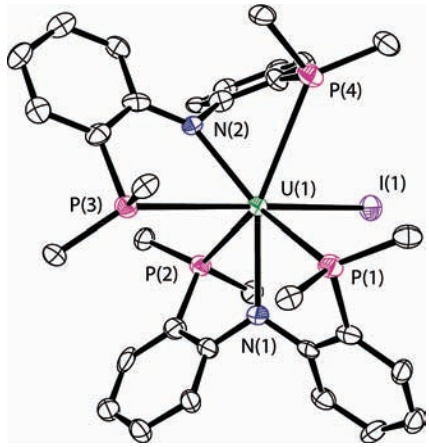

Figure 4. Molecular structure of complex **12** with thermal ellipsoids projected at the 50% probability level. Hydrogen atoms and methyl groups have been omitted for clarity. Selected bond distances (Å) and angles (deg): U(1)−N(1) 2.439(5), U(1)−N(2) 2.376(5), U(1)−P(1) 3.076(2), U(1)−P(2) 3.063(2), U(1)−P(3) 3.316(2), U(1)−P(4) 3.197(2), U(1)−I(1) 3.109(1), P(1)−U(1)−N(1) 65.22(14), P(2)−U(1)−N(1) 63.43(14), P(3)−U(1)−N(2) 60.29(13), P(4)−U(1)−N(2) 61.86(13), I(1)−U(1)−P(1) 87.40(4), I(1)−U(1)−P(4) 76.87(4).

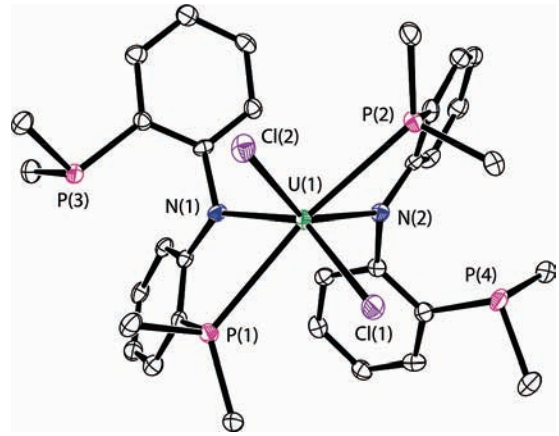

Figure 5. Molecular structure of complex **13** with thermal ellipsoids projected at the 50% probability level. Hydrogen atoms and methyl groups have been omitted for clarity. Selected bond distances (Å) and angles (deg): U(1)−N(1) 2.290(3), U(1)−N(2) 2.279(3), U(1)−P(1) 2.996(1), U(1)−P(2) 3.004(1), U(1)−Cl(1) 2.590(1), U(1)−Cl(2) 2.576(1), P(1)−U(1)−N(1) 64.20(9), P(2)−U(1)−N(2) 64.58(9), Cl(1)−U(1)−Cl(2) 101.37(4), Cl(1)−U(1)−P(1) 78.89(3), Cl(2)−U(1)−P(2) 81.04(3).

in symmetry observed for **12** is due to the decoordination of at least one arm of the phosphine donor in solution.

This premise is supported by the solid-state molecular structure of complex **12**, which is given in Figure 4. Although the two PNP ligands coordinate to the uranium(III) metal center in a κ^3-(*P*,*N*,*P*) fashion, they present very different features. The first PNP ligand (identified by P(1), N(1) and P(2)) is identical to the PNP ligand in the mono(PNP) complex **7** and features the same U−P and U−N bond distances. Moreover, as observed in complexes **7**−**11**, the uranium center lies in the (P(1), N(1), P(2)) plane with δ_{PUNP} = 171.9° and *d*(U−PNP) = 0.20 Å. In contrast, the second PNP ligand (identified by P(3), N(2) and P(4)) is highly twisted with the metal being out of the (P,N,P) plane of the ligand, with δ_{PUNP} = 128.3° and *d*(U−PNP) = 2.00 Å. This situation is not observed in complexes **7**−**11** nor in the known transition metal and lanthanide PNP complexes and demonstrates the ability of the PNP ligand to adopt multiple coordination geometries.[64] Interestingly, this geometry alters the U−P and U−N bond distances. The U−N(2) bond length of 2.376(5) Å is considerably shorter than that for U−N(1) (2.439(5) Å). In addition, U−P(3) = 3.316(2) Å and U−P(4) = 3.197(2) Å are about 6% longer than the U−phosphine bond distances observed for U−P(1) (3.076(2) Å) and U−P(2) (3.063(2) Å). Clearly, these data reflect increased steric hindrance around the metal center, which weakens the U−phosphine interactions (where the steric crowding is the greatest) and reinforces the U−amide bond for one of the PNP ligands. This is in agreement with the absence of any coordinated solvent in the coordination sphere of the metal.

As depicted in Scheme 3, the reaction between UCl_4 and 2 equiv of (PNP)K (**6**) at room temperature for 2 days also yields a bis(PNP) complex (**13**) in excellent yield after workup. The new uranium(IV) dichloride complex was characterized by a combination of ^{1}H and ^{31}P{^{1}H} NMR spectroscopy and X-ray diffraction. The solid state structure of **13** is shown in Figure 5 and reveals a new κ^2-(*P*,*N*) coordination motif of PNP binding to the uranium(IV) center. The U−N and U−P bond distances (U(1)−N(1) 2.290(3), U(1)−N(2) 2.279(3), U(1)−P(1) 2.996(1), U(1)−P(2) 3.004(1)) are in agreement with those found in the U^{IV} complex **9** (Table 2). To the best of our knowledge, κ^2-(*P*,*N*) coordination of a PNP ligand has not been observed to date for any transition metal or lanthanide PNP complex. Contrary to previous assumptions, this κ^2-(*P*,*N*) coordination mode demonstrates the ability of the PNP ligand to act as a hemilabile ligand and further confirms our proposed analysis of the solution structure of complex **12**; that being, decoordination of a PNP phosphine arm.

To determine whether this coordination mode is maintained in solution, variable temperature ^{1}H and ^{31}P{^{1}H} experiments were performed on a THF-d_8 solution of complex **13**. At −50 °C, the ^{31}P{^{1}H} spectrum consists of two singlets at δ 1401.1 and 50.3 ppm revealing the presence of uncoordinated phosphine donors.[65] The integration pattern for the ^{1}H signals is consistent with a complex of overall C_s or C_2 symmetry, pointing to a structure equivalent to that observed in the solid state (Figure 5) with two κ^2-(*P*,*N*)-coordinated PNP ligands. At higher temperature (+50 °C), the same structure could be derived from the ^{1}H and ^{31}P{^{1}H} spectra.

Structural Evaluation of the Mono and Bis(PNP) Uranium Complexes. Comparison of the X-ray structures of the mono and bis(PNP) complexes (**7**, **9**, **10**, **12**, and **13**) reveals that the U-phosphine bond distances are not noticeably influenced by the oxidation state of the metal center or the number of coordinated PNP units. The same finding

(64) A similar situation (δ_{PUNP} = 139.8°) was observed for the thalium complex (PNP)Tl, see: DeMott, J. C.; Basuli, F.; Kilgore, U. J.; Foxman, B. M.; Huffman, J. C.; Ozerov, O. V.; Mindiola, D. J. *Inorg. Chem.* **2007**, *46*, 6271–6276.

(65) The large difference in chemical shifts between these two signals precluded the determination of their relative integration by ^{31}P{^{1}H} NMR.

Scheme 4. Geometric Differences between the C_5Me_5 and PNP Ligands upon Coordination to Uranium

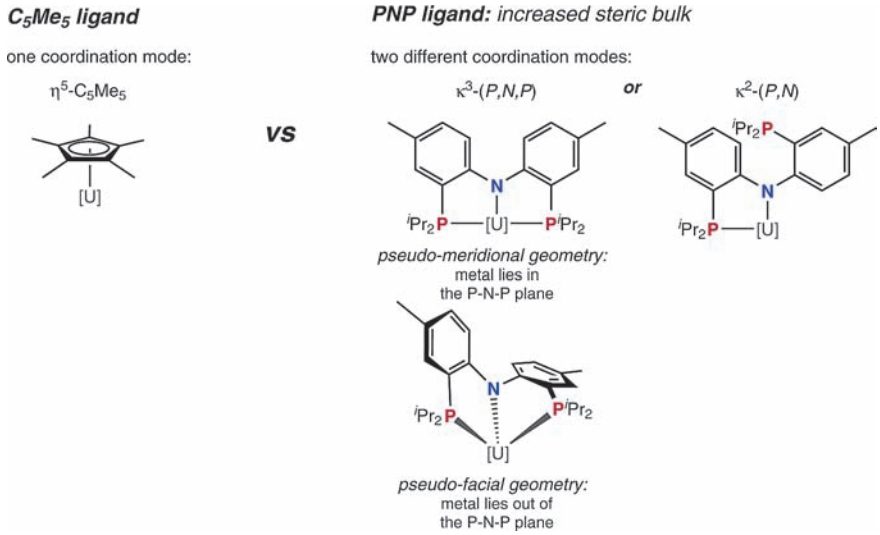

prevails for the $U-N_{amide}$ bond lengths, which are more sensitive to the total coordination number of the complex as seen for the mono(PNP) uranium (IV) complexes **9** (U−N(1) = 2.343(7) Å) and **10** (U−N(1) = 2.411(3) Å), which have coordination numbers of 7 and 8, respectively. Clearly, the oxidation state of the metal center cannot be deduced from these metric parameters.

Further, the electronic influence of replacing the C_5Me_5 ligands in **1**−**4** with PNP to yield **7**, **9**, **10**, **12**, and **13** cannot be simply tracked by comparing the U−Cl or U−I bond distances. Therefore, the structural data do not allow a detailed comparison between the C_5Me_5 and PNP ligand or their impact on the electronic structure of the corresponding uranium complexes, which were investigated using electronic absorption spectroscopy and electrochemistry (vide infra).

The κ^3-(*P*,*N*,*P*) coordinated PNP ligand was found to be more bulky than the η^5-C_5Me_5. Scheme 4 shows that the C_5Me_5 and PNP coordination motifs do present interesting geometric discrepancies that should lead to different chemical behaviors. The C_5Me_5 ligand exhibits a single η^5-coordination mode upon coordination to actinides, and the related bis(C_5Me_5) complexes generally adopt a bent metallocene structure, with the exception of a few recent examples of uranium linear metallocene complexes.[66,67] In contrast, the present work demonstrates that the PNP framework is more versatile and able to adopt two different coordination modes: κ^2-(*P*,*N*) and κ^3-(*P*,*N*,*P*) with *pseudo*-meridional or *pseudo*-facial geometries.

Electrochemistry and Electronic Spectroscopy. To assess the electronic structure in this new class of low- and midvalent uranium complexes, we have obtained voltammetric data for complexes **3**, **12** and **13**, and UV−visible-near-infrared electronic absorption spectral data for complexes **3**, **7**, **10**−**13**, and compared these data to previously published results for analogous C_5Me_5 complexes.[68] Previous work, principally on the bis(C_5Me_5) systems, has demonstrated that metal-centered redox potentials, electronic transition energies, and electronic transition intensities all provide insight into the ligand-derived variations in the electron density at the metal center, the magnitude of the crystal-field induced splitting of the 5f electronic manifold derived from the $5f^2$ (U^{4+}) and $5f^3$ (U^{3+}) valence electronic configurations, and the extent of covalency in the metal−ligand

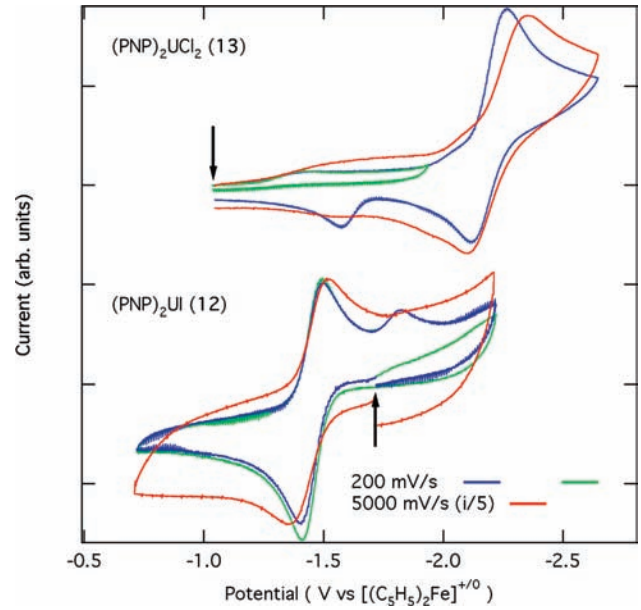

Figure 6. Cyclic voltammograms for $(PNP)_2UI$ (**12**) and $(PNP)_2UCl_2$ (**13**) in ∼0.1 M $[Bu_4N][B(1,3\text{-}(CF_3)_2\text{-}C_6H_3)_4]$/THF solution at a Pt working electrode. The vertical arrows indicate the rest potentials of each solution.

Table 3. Comparison of U^{IV}/U^{III} Redox Potentials for Homologous PNP vs C_5Me_5 Complexes[a]

complex	$E_{1/2}$ [U^{IV}/U^{III}] (V)	$\lvert\Delta E_{1/2}(1)\rvert$[b] (mV)	$\lvert\Delta E_{1/2}(2)\rvert$[c] (mV)
$(PNP)_2UCl_2$ (**13**)	−2.19		
		340	
$(C_5Me_5)_2UCl_2$ (**4**)[d]	−1.85		
			720 (PNP),730 (C_5Me_5)
$(PNP)_2UI$ (**12**)	−1.47		
		350	
$(C_5Me_5)_2UI(THF)$ (**3**)	−1.12		

[a] Potentials vs $[(C_5H_5)_2Fe]^{+/0}$ in ∼0.1 M $[Bu_4N][B(C_6F_5)_4]$/THF. [b] $\Delta E_{1/2}(1) = E_{1/2}$(PNP complex) − $E_{1/2}$(C_5Me_5 complex). [c] $\Delta E_{1/2}(2) = E_{1/2}(U^{IV}$ complex) − $E_{1/2}(U^{III}$ complex). [d] Data from ref 68.

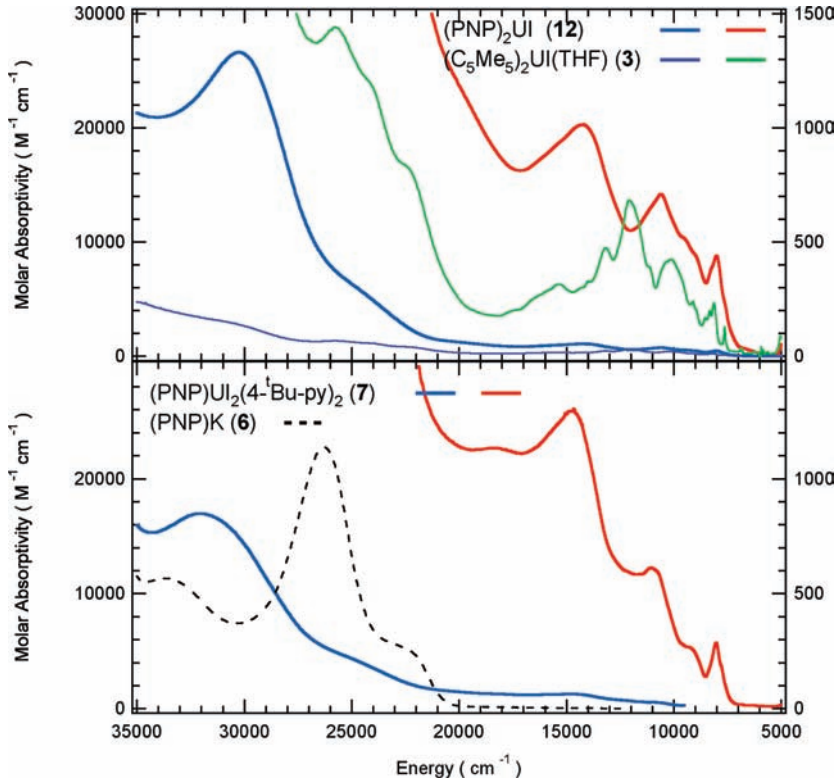

Figure 7. UV−visible-near IR electronic absorption spectral data for toluene solutions of $(C_5Me_5)_2UI(THF)$ (**3**), (PNP)K (**6**), $(PNP)UI_2(4\text{-}^tBu\text{-}py)_2$ (**7**), and $(PNP)_2UI$ (**12**). The left ordinate scale pertains to the UV−visible region (blue, purple, and black spectra) and the right ordinate scale to the near-IR region (red and green spectra).

bonding. By comparison of data for structural homologues in which the C_5Me_5 framework is replaced by a PNP framework, an evaluation of changes in electronic structural properties derived from the framework change should be possible, and correlations in molecular/electronic structure should enable greater insight and predictive capability regarding trends in complex stability and reactivity patterns. In general, we find that the electrochemical and spectroscopic behavior for analogous C_5Me_5 and PNP complexes of U^{III} and U^{IV} is quite similar, albeit with some important perturbations described in detail below.

Cyclic and square-wave voltammetric data were obtained for bis(PNP) complexes of uranium(III) (**12**) and uranium(IV) (**13**) in ∼0.1 M $[Bu_4N][B(1,3\text{-}(CF_3)_2\text{-}C_6H_3)_4]$/THF solution at a Pt working electrode. (All potentials are referenced to the $[(C_5H_5)_2Fe]^{+/0}$ couple.) Typical cyclic voltammograms are illustrated in Figure 6, and the potential data determined from the peaks in the square-wave voltammograms (not shown) are summarized and compared to similar data for the C_5Me_5 systems in Table 3. An attempt was also made to collect voltammetric data for mono(PNP) complexes **7** and **11**, but both complexes degraded completely as evidenced by loss of solution color within a few minutes in the solvent/supporting electrolyte solution. The defining characteristic in the voltammetry of complexes **12** and **13** is a chemically reversible wave attributed in both cases to the U^{IV}/U^{III} redox transformation. For both systems there is also evidence for a chemical process coupled to this metal-based redox transformation as evidenced by the new cathodic peak in the voltammograms of **12** at ∼−1.9 V and the new anodic peak in the voltammograms of **13** at ∼−1.6 V. This extra feature is only observed in conjunction with the metal-based couple as illustrated in the green traces in Figure 6, and the current magnitude of the extra feature is diminished at faster scan rates as indicated in the red traces; both observations are consistent with the assignment of this extra feature to a coupled chemical process. Given the hemilability of the PNP ligand noted above, it is plausible that this new product formed in minor amounts in conjunction with the redox transformation is a complex of different PNP denticity that has slightly different redox energetics. As gleaned from the ^1H and ^{31}P NMR studies on complexes **12** and **13**, it is indeed likely that upon reduction of **13** the coordination mode of one PNP ligand changes from κ^2-(*P*,*N*) to κ^3-(*P*,*N*,*P*) to stabilize the larger uranium(III) center (a decrease of the denticity of one PNP ligand is conversely expected upon oxidation of **12**). Interestingly, this coordination of a soft donor (P) leads to an ∼150−300 mV shift of the U^{IV}/U^{III} couple to more positive potentials, therefore stabilizing the uranium(III) oxidation state. The only other voltammetric features (not illustrated in the data in Figure 6) found in these studies are two irreversible oxidation waves in the data for **13** at ∼−0.1 and 0.2 V. These are ascribed to oxidations of the coordinated chloride ions. The electrochemical behavior for the bis(PNP) complexes **12** and **13** is analogous to that for the bis(C_5Me_5) congeners **3** and **4** in that the principal redox process is a reversible U^{IV}/U^{III} couple (Table 3), and no other metal-based redox transformation (e.g., U^V/U^{IV}) are observed.

Variations in these metal-based redox potentials for the same U^{IV}/U^{III} oxidation state transformation primarily reflect the differing degrees of electron density at the metal center

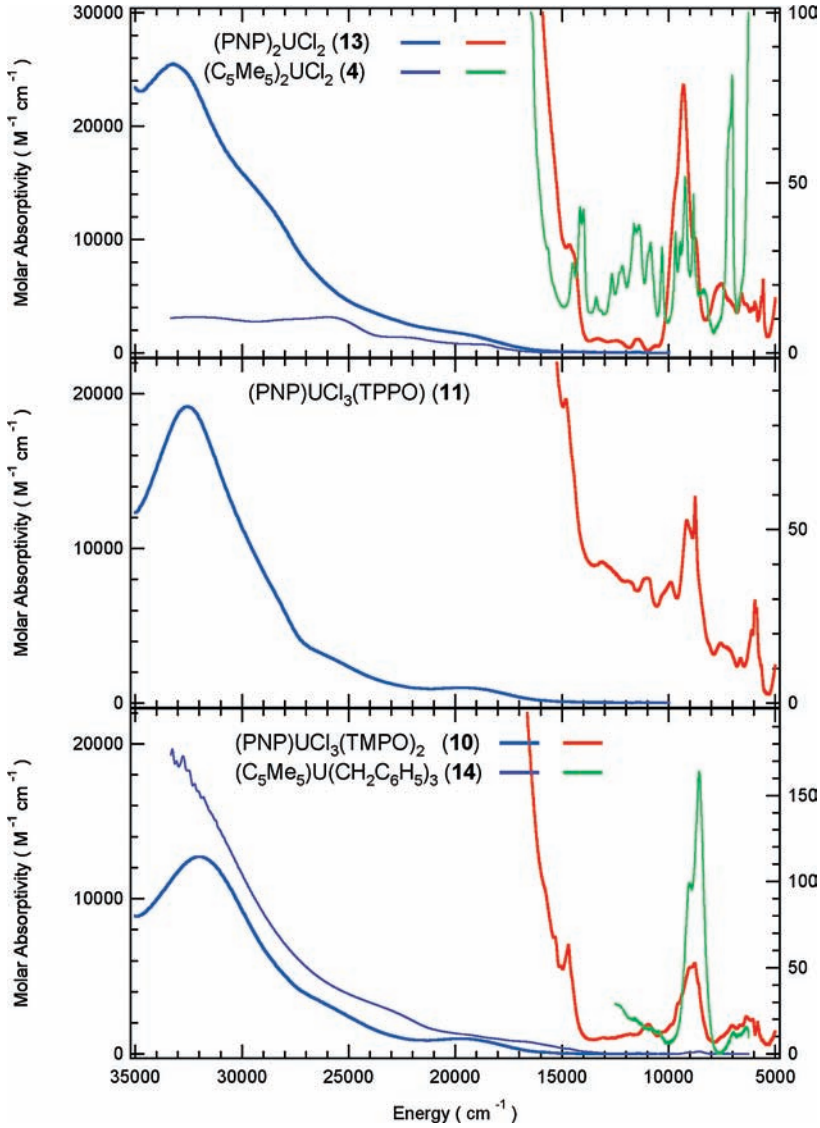

Figure 8. UV−visible-near IR electronic absorption spectral data for toluene solutions of $(C_5Me_5)_2UCl_2$ (**4**), $(PNP)UCl_3(TMPO)_2$ (**10**), $(PNP)UCl_3(TPPO)$ (**11**), $(PNP)_2UCl_2$ (**13**), and $(C_5Me_5)U(CH_2C_6H_5)_3$ (**14**). The left ordinate scale pertains to the UV−visible region (blue, purple, and black spectra) and the right ordinate scale to the near-IR region (red and green spectra). Data for **14** are reproduced from ref 68.

as a result of changes in the electron-donating (withdrawing) ability of the ligand(s) and the number of such ligands. The more substantial energetic effect for both bis(PNP) and bis(C_5Me_5) systems results from the replacement of a single iodide ligand by two chloride ligands. In both systems, this structural change shifts the U^{IV}/U^{III} couple by ~700 mV ($\Delta E_{1/2}(2)$, Table 3) to more negative potentials as a result of stabilization of the higher oxidation state (or, conversely, destabilization of the lower oxidation state).

The influence of the bis(PNP) framework relative to the bis(C_5Me_5) framework can be seen in the $\Delta E_{1/2}(1)$ values in Table 3. The energetic consequence of this structural change for both the uranium(III) iodide and the uranium(IV) dichloride is a ~350 mV shift of the U^{IV}/U^{III} couple to more negative potentials on substitution of bis(C_5Me_5) by bis(PNP). This leads to the somewhat counterintuitive conclusion that the PNP ligand induces greater electron density at the metal center than does the C_5Me_5 ligand. The overall comparability in the magnitude of these $\Delta E_{1/2}(1,2)$ values points to the importance of electrostatic effects in determining the redox energetics in these systems dominated by σ-donor and/or dative metal−ligand interactions.

The electronic absorption spectra in the UV−visible region ($E > \sim 15{,}000\ cm^{-1}$) for the PNP complexes of uranium(III) (Figure 7) and uranium(IV) (Figure 8), as well as that of the simple ligand salt, (PNP)K (**6**) (Figure 7, bottom panel), are all quite similar and appear to be dominated by PNP ligand-based transitions that are shifted to higher energy in the uranium complexes than in the simple ligand anion spectrum. The assignment of these broad, high intensity transitions in the uranium complexes to PNP ligand-based processes is supported by the similarity in the data for the free ligand anion, and by comparison to the UV−visible data for most of the C_5Me_5 congeners for which the UV−visible transition intensities are diminished 5−10 times relative to that in the PNP systems suggesting very different origins. The notable exception to this intensity difference is found for $(C_5Me_5)U(CH_2C_6H_5)_3$ (**14**), for which the intensities in the UV−visible bands are comparable to those in this spectral region for the PNP complexes. In contrast, the electronic

spectral data in the near IR (NIR) spectral region for the PNP systems show a good qualitative correlation with the data for their C_5Me_5 congeners. This region is dominated by f-f transitions derived from the $5f^3$ (U^{3+}) and $5f^2$ (U^{4+}) valence electronic configurations. The density of ligand-field states from which these NIR transitions derive is very large for both valence electronic configurations,[69] and specific assignments are not possible. There are, however, some noteworthy trends in both energies and intensities across the comparative series illustrated in Figures 7 and 8.

The energies and relative intensities of the f-f transitions for the two uranium(III) PNP complexes (Figure 7, complexes **7** and **12**) are quite similar. The NIR spectrum for the $(C_5Me_5)_2U^{III}$ congener (**3**) is similar to that of the PNP analogues, although there does appear to be a compression of the spectral bands in the region from ~10,000−5,000 cm^{-1} into a narrower energy window for **3** suggesting that the ligand-field splitting is somewhat less in the C_5Me_5 complex than in the PNP complexes (as would be expected based on the electrochemical result demonstrating that PNP donates greater electron density than C_5Me_5). The intensities in the f-f bands for all uranium(III) complexes are also comparable, and do not depend to a large degree on the structural framework (PNP vs C_5Me_5). Similar energetic and intensity arguments can be made regarding the comparisons in the NIR region for the uranium(IV) systems (Figure 8). In particular, although there are clearly differences in the splitting of the f-f bands for the different ligand sets, there are no wholesale variations in the intensities for the PNP versus C_5Me_5 systems.

Conclusions

The first actinide complexes of the bis[2-(diisopropylphosphino)-4-methylphenyl]amido ligand (PNP) have been prepared and have demonstrated new coordination modes for this ligand set. The PNP scaffold is able to stabilize both uranium(IV) and uranium(III) halide complexes, namely $(PNP)UI_2$(4-tert-butylpyridine)$_2$ (**7**), $[(PNP)UCl_3]_2$ (**8**), $(PNP)UCl_3$(THF) (**9**), $(PNP)UCl_3(TMPO)_2$ (**10**), and $(PNP)UCl_3$(TPPO) (**11**). For the first time, bis(PNP) complexes have been accessed giving $(PNP)_2UI$ (**12**) and $(PNP)_2UCl_2$ (**13**). Interestingly, these complexes reveal that new coordination modes are available for the PNP ligand, with a denticity of two (κ^2-(*P*,*N*)) or three (κ^3-(*P*,*N*,*P*)) and two different geometries (*pseudo*meridional vs *pseudo*facial) for the κ^3-(*P*,*N*,*P*) coordination mode.

The influence of replacing the C_5Me_5 ligands in **1**−**4** with PNP (**7**, **9**, **11**−**13**) on the geometry and electronic structure of the complexes was investigated using X-ray analysis, electronic absorption spectroscopy, and electrochemistry. The PNP ligand was shown to provide a more sterically congested environment in complexes **7**−**13**. Both the bis(C_5Me_5) and bis(PNP) systems present a chemically reversible wave corresponding to the U^{IV}/U^{III} redox transformation (for **3**, **4**, **12**−**13**). However, a ~350 mV shift of this couple to more negative potentials was observed on substitution of the bis(C_5Me_5) by the bis(PNP) framework, therefore pointing to greater electronic density at the metal center in the PNP complexes. The UV−visible regions of the electronic spectra for the mono(PNP) and bis(PNP) complexes are dominated by PNP ligand-based transitions. The near IR region in complexes **1**−**4** and **7**, **9**, **11**−**13** is dominated by f-f transitions, and although both ligand sets exhibit similar intensities, a somewhat greater ligand-field splitting was noticed for the PNP system, consistent with its higher electron donating ability. Studies aimed at exploiting the novel electronic and geometric features provided by these PNP uranium halide systems are currently underway to support novel structures and promote new reactivity patterns for the actinide series.

Acknowledgment. For financial support of this work, we acknowledge LANL (Director's PD Fellowship to T.C.), and the Division of Chemical Sciences, Office of Basic Energy Sciences, Heavy Element Chemistry program. We are also thankful to Prof. Oleg V. Ozerov (Brandeis University) for providing the initial samples of (PNP)H (**5**) used in this work. This work was carried out under the auspices of the National Nuclear Security Administration of the U.S. Department of Energy at Los Alamos National Laboratory under Contract DE-AC5206NA25396.

Supporting Information Available: Crystallographic data in CIF file format. This material is available free of charge via the Internet at http://pubs.acs.org.

IC802061X

(66) Maynadie, A.; Berthet, J. C.; Thuery, P.; Ephritikhine, M. *J. Am. Chem. Soc.* **2006**, *128*, 1082–1083.
(67) Maynadie, J.; Barros, N.; Berthet, J.-C.; Thuery, P.; Maron, L.; Ephritikhine, M. *Angew. Chem., Int. Ed.* **2007**, *46*, 2010–2012.
(68) Morris, D. E.; Da Re, R. E.; Jantunen, K. C.; Castro-Rodriguez, I.; Kiplinger, J. L. *Organometallics* **2004**, *23*, 5142–5153.
(69) (a) Carnall, W. T.; Crosswhite, H. M. *Optical Spectra and Electronic Structure of Actinide Ions in Compounds and in Solution*; Argonne National Laboratory: Argonne, IL, 1985; ANL-84−90. (b) Liu, G.; Beitz, J. V. In *The Chemistry of the Actinide and Transactinide Elements*, 3rd ed.; Morss, L. R., Edelstein, N. M., Fuger, J., Eds.; Springer: Dordrecht, The Netherlands, 2006: Vol. *3*, pp 2013−2111.